Responses to Reviewers' Comments for Manuscript egusphere-2025-4190

Assessment of transparent exopolymer particles in the Arctic Ocean implemented into the coupled ocean–sea ice–biogeochemistry model FESOM2.1–REcoM3

Addressed Comments for Publication to

Geoscientific Model Development

by

Moritz Zeising [1], Laurent Oziel [1], Silke Thoms [1], Özgür Gürses [1], Judith Hauck [1,2], Bernd Heinold [3], Svetlana N. Losa [1,4], Manuela van Pinxteren [3], Christoph Völker [1], Sebastian Zeppenfeld [3], and Astrid Bracher [1,5]

[1] Alfred Wegener Institute Helmholtz Center for Polar and Marine Research, Bremerhaven, Germany
[2] University of Bremen, Bremen, Germany
[3] Leibniz Institute for Tropospheric Research, Leipzig, Germany
[4] Shirshov Institute of Oceanology, Russian Academy of Sciences, Moscow, Russia
[5] Institute of Environmental Physics, University of Bremen, Bremen, Germany

Dear Chia-Te Chien,

Please find enclosed the revised version of our previous submission entitled "Assessment of transparent exopolymer particles in the Arctic Ocean implemented into the coupled ocean–sea ice– biogeochemistry model FESOM2.1–REcoM3" with manuscript number egusphere-2025-4190. We would like to thank you and the reviewers for the valuable comments which help improving the quality of our manuscript. We have carefully addressed the reviewers' comments. A summary of main modifications and a detailed point-by-point response to the comments from Reviewers 1 and 2 are given below.

Sincerely,

Moritz Zeising

on behalf of all authors

Note: To enhance the legibility of this response letter, all the reviewers' comments are typeset in blue boxes followed by our reply. Rephrased or added sentences in the manuscript are typeset in grey boxes. The respective parts in the manuscript are highlighted to indicate changes. When referred in the text, line numbers point to the revised version of the manuscript. Figure numbers are referenced likewise to the revised manuscript and linked to the automated LaTeX numbering in this response letter.

The LaTeXtemplate for this response letter was provided by Karl-Ludwig Besser (https://github.com/klb2/).

Authors' Response to Reviewer 1

General Comments. The paper by Zeising and co-authors, titled "Assessment of transparent exopolymer particles in the Arctic Ocean implemented into the coupled ocean–sea ice–biogeochemistry model FESOM2.1–REcoM3", describes the new implementation of PCHO and TEP tracers and respective processes in a global ocean BGC model, which is calibrated for the Arctic Ocean. The model was integrated for 1958-2019 period where the results from the last three decades is analyzed. In addition to evaluating the performance of the simulated PCHO and TEP, they present the mean states and spatial distribution of the simulated phytoplankton-related carbon state variables, including the seasonal cycle, and comparison with observational-based estimates. It is nicely written and easy to follow with clear figures to illustrate key messages the authors try to convey. As a model description, the paper contains sufficient details and result presentations. I have a few comments that hopefully the authors can address to further improve the paper.

Response: Thank you for your feedback. We appreciate your support for our manuscript on the assessment of transparent exopolymer particles (TEP) in the ocean biogeochemistry model FESOM2.1–REcoM3. We have carefully addressed all the issues item by item as follows. We have made the necessary revisions and hope that we have addressed all of the concerns raised.

Comment 1

Impacts of adding these new processes and state variables. The motivation is well outlined in the introduction, nevertheless, how do these new processes change the carbon/nutrient cycling/export production/PP/etc., as compared to the model's reference configuration without these new tracers, are not so clear after reading the paper. The readers should get some insights whether these processes are indeed important and/or worth implementing in other models.

Response: Thank you for the comment. We agree that the manuscript can profit from a comparison to a control run. Therefore, we added the comparison to a control run

conducted by us to several sections of the manuscript. In the Methods, the control run is formally introduced (L. 117–118):

> Additionally, a FESOM2.1–REcoM3 control run was conducted using the same setup as described above but without the additional organic carbon process descriptions for PCHO and TEP.

For the general model assessment in terms of primary production, we added a comparison of the Total Chlorophyll *a* (TChla) concentrations of the simulation with the control run and the Copernicus remote-sensing data product to Fig. 3 (Fig. 3 in this document). In the Results Section, we added a short figure description in Section 3.1 (L. 275–291):

> The phytoplankton biomass in the surface Arctic Ocean in terms of TChla is depicted in Fig. 3, where the FESOM2.1–REcoM3 simulation is compared to the CMEMS Arctic satellite re-analysis product and a control run without TEP. The data is averaged over the years 2000 to 2019 (as a mean model state) for the months May to September when satellite data are available. The CMEMS TChla product shows no coverage of the central Arctic Ocean due to the satellite sensors configuration not enabling observations at these high latitudes (Fig. 3 panel a). In the Barents, Kara, and Laptev Seas, TChla ranges from 0.5 to 5 $\mathrm{mg\,m^{-3}}$, with peaks of up to 15 $\mathrm{mg\,m^{-3}}$ close to the coastline. In the East Siberian, Chukchi, and Beaufort Seas, the concentration of TChla is lower, ranging from 0.1 to 1 $\mathrm{mg\,m^{-3}}$, also with very high concentration close to the coast. The standard deviation of TChla from the CMEMS TChla product is mostly lower than 0.5 $\mathrm{mg\,m^{-3}}$. However, it increases to more than 2 $\mathrm{mg\,m^{-3}}$ along the coastline (Fig. 3 panel d). In the control simulation of FESOM2.1–REcoM3 without TEP, TChla concentration range from below 0.2 $\mathrm{mg\,m^{-3}}$ in the central Arctic Ocean to approximately 2 $\mathrm{mg\,m^{-3}}$ in the Fram Strait and Chukchi Sea, reaching even values of 3 $\mathrm{mg\,TChla\,m^{-3}}$ close to the coast of the Russian shelves. The FESOM2.1–REcoM3 including TEP simulates highest TChla concentrations of up to 6 $\mathrm{mg\,m^{-3}}$ along the Russian coast and in other shelf seas between 0.5 and 3 $\mathrm{mg\,m^{-3}}$ (Fig. 3 panel c). In the Fram Strait, TChla range from 1 to 3 $\mathrm{mg\,m^{-3}}$ with highest concentration in its central part, while in the central basins of the Arctic Ocean, TChla is generally low, with concentrations of up to 0.8 $\mathrm{mg\,m^{-3}}$. Compared to the control run without the TEP implementation, TChla concentrations are slightly elevated by 0.2 to 1 $\mathrm{mg\,m^{-3}}$ in

the Fram Strait, in the Beaufort Gyre, and in the Chukchi Sea (Fig. 3 panel f). In the coastal areas of the Russian shelves, the simulated TChla is predominantly lower compared to the remote sensing product.

In the Discussion Section 4.1, we added more details on the TChla of the model run compared to the control run, to the CMEMS remote-sensing product, and to observations. We restructured and enriched the whole first part of the section (L. 404–454):

In terms of Arctic-wide TChla, the FESOM2.1–REcoM3 output is evaluated with the remote-sensing product provided by CMEMS and with various in situ datasets. Generally, the model run aligns with the compiled remote-sensing data of CMEMS TChla (Fig 3). The control run without the TEP implementation underestimates the TChla concentration in large parts of the Barents Sea and on the Arctic shelves, which was reported in Gürses et al. (2023) as well. Overall, the model run including TEP performs in better agreement with CMEMS. Still in the Chukchi Sea and the Beaufort Gyre, as well as in the Fram Strait, the model run overestimates TChla compared to both the control run and CMEMS. Climatological monthly maps of TChla are included as Supplementary Fig. A2.

As such, this pattern of the FESOM2.1–REcoM3 model run compares well to the results from Nöthig et al. (2020) and also to other observations. The generally higher TChla concentrations in the model run compared to the control might reflect the higher turnover of phytoplankton biomass: TEP increases the aggregation of phytoplankton to detritus, which partly gets remineralized, replenishes nutrients to the seawater, and enables new build-up of phytoplankton biomass. In accordance with this hypothesis, we observe higher nutrient concentrations in the central Arctic Ocean, in the Beaufort Sea, and in the Chukchi Sea compared to the control run (Supplementary Fig. A3). However, we have not yet investigated the influence of TEP on the nutrient dynamics in the Arctic Ocean any further.

Evaluating the TChla patterns in more regional detail, we start with the eastern Fram Strait. Both CMEMS and the model run present the beginning of the phytoplankton bloom in May which prevails with TChla of approximately 1–3 $\mathrm{mg m^{-3}}$ through the summer months (Supplementary Fig. A4 and A2 panel a). In the eastern Fram Strait, in situ measurements of Nöthig et al. (2020) result in a median vertically integrated concentration of 44 $\mathrm{mg\,m^{-2}}$ (0–100 m depth), and in

the Barents Sea of 42 mg m^{-2} which agree with simulated median concentrations of 40.4 and 33.8 mg m^{-2}, respectively (Fig. 4 panel a). The results are also in line with the two-year round mooring observations at the long-term ecological research observatory HAUSGARTEN in the eastern Fram Strait with simulated TChla concentration reaching up to 5 mg m^{-2} in the upper 30 m compared to 7 mg m^{-2} in measurements (von Appen et al., 2021). In the MIZ, especially in the area of Fram Strait, phytoplankton growth is expected to be highest, as the sea-ice breaks up, light availability is increased and the water column is stratified (Cherkasheva et al., 2014; Nöthig et al., 2020). Likewise in the western part of Fram Strait and in the Siberian seas, the lower amount of simulated TChla matches in situ data for these regions spanning 13 to 26 mg m^{-2} (Nöthig et al., 2020; Piontek et al., 2021). In the Chukchi and Beaufort Seas, the simulated TChla concentration itself (and the difference between FESOM2.1–REcoM3 and CMEMS) is generally low (less than 1.5 mg m^{-3}, Fig. 3 panel c and f). However, the timing of the phytoplankton bloom differs from May in CMEMS to June–July in the model run (Supplementary Fig. A4 and A2 panel a). Other observations from in situ data and satellite-derived products draw a diverse picture in these seas with massive under-ice blooms in the Chukchi Sea with high TChla concentration of up to 30 mg m^{-3} (Arrigo et al., 2014), and low (0.02–0.25 mg m^{-3}) TChla concentration in the northern Chukchi and Beaufort Seas (Jung et al., 2022; Park et al., 2019). In the central Arctic Ocean, vertically integrated TChla is low in both simulation (integrated over 0–100 m water depth, median 0.01 mg m^{-2}) and measurements (7–8 mg m^{-2}). No coverage by the remote-sensing product by CMEMS is available.

As such, the higher TChla concentration of the FESOM2.1–REcoM3 model run might be a better fit to observation data than CMEMS. One explanation for the observed difference may be that CMEMS sampled far less days than are simulated by FESOM2.1–REcoM3. Schourup-Kristensen et al. (2018) explain lower TChla in the simulation by full spatial and temporal coverage whereas only open-water productive regions are accessible from remote-sensing measurements. However, Assmy et al. (2017) suggest that remote-sensing products don't capture the phytoplankton bloom forming under thin ice or melt ponds, therefore often result in too low TChla estimates. A likely explanation for the higher simulated median TChla concentration in several regions and higher variability in comparison to Nöthig et al. (2020) might be the consideration of up to 62k data points in

the regional subsets (Fig. 4 panel a) compared to only a few hundred in Nöthig et al. (2020), where the in situ sampling is mostly limited to one campaign each spring-summer season. Additionally, the evaluated regions of the model run contain the whole continental shelve grid points, whereas the in situ measurements are located mostly in the northern parts of the shelf seas (Nöthig et al., 2020).
However, in the coastal areas of the shelf areas (the Barents, Kara, and Laptev Seas and close to the Canadian coast) FESOM2.1–REcoM3 model run highly underestimates TChla concentrations provided by CMEMS (Fig. 3 panel c). There, CMEMS is error-prone (high standard deviation, Fig. 3 panel d), most likely due to the very high colored dissolved organic matter and total suspended matter concentrations, which have not been sufficiently accounted for in the retrieval process. This results in a significant overestimation of TChla (Copernicus Marine Service, 2023; Heim et al., 2014; Schourup-Kristensen et al., 2018). Also other remote-sensing products overestimate TChla on the Arctic shelves (Mustapha et al., 2012).

Comment 2

Assuming similar baseline experiments exist but without the new improvements, some figures or performance metrics could be useful to have. For instance, a climatological seasonal vertical profile of nutrients from models with and without this modification (compared with observations) could be interesting to see.

Response: Thank you for the comment. We agree that a nutrient comparison could be valuable. Thank you for suggesting seasonal profiles, we decided to add a comparison of the nutrient concentrations as maps because this provides a good overview on the entire Arctic Ocean. The implementation of the additional organic carbon equations result in DIN concentrations elevated by 1–2 $\mathrm{mmol\,m^{-3}}$ in the central Arctic Ocean, in the Beaufort Sea, in the Chukchi Sea, and in the Canadian Archipelago, whereas only a minor difference is found in the Fram Strait and Barents Sea (Fig. A3/ Fig. 7 in this document, panel c). The control run results in higher DIN concentrations only at the river mouths. Regarding DSi, the comparison of the model run to control does not yield large differences ($< 20\%$) except for higher DSi concentration in the inflow of the Lena river in the control. Similarly for DFe, the differences are small except for an increase

of DFe concentration in the model run by approximately 25% in the western Chukchi Sea/Lena river inflow. Generally, the model run containing TEP agrees better to the World Ocean Atlas dataset, which suggests a DIN concentration of 5–10 $\mathrm{mmol\,m^{-3}}$ in the Arctic Ocean (Garcia et al., 2019a,b).

As outlined above, we assume that the higher aggregation rate due to TEP could increase the remineralization of these nutrients, which we have shortly included in the manuscript Discussion Section 4.1 (L.411–417):

> The generally higher TChla concentrations in the model run compared to the control might reflect the higher turnover of phytoplankton biomass: TEP increases the aggregation of phytoplankton to detritus, which partly gets remineralized, replenishes nutrients to the seawater, and enables new build-up of phytoplankton biomass. In accordance with this hypothesis, we observe higher nutrient concentrations in the central Arctic Ocean, in the Beaufort Sea, and in the Chukchi Sea compared to the control run (Supplementary Fig. A3). However, we have not yet investigated the influence of TEP on the nutrient dynamics in the Arctic Ocean any further.

Comment 3

How much of the 662Pg DOC (L17) are PCHO based on your model simulation? How much are converted to POC or what is the new POC export rate? Can you stipulate how future climate change may alter this and the broader ocean carbon cycle?

Response: Thank you for the comment. It is difficult to determine, which amount of DOC is exactly a combined carbohydrate because of the large molecular variety of compounds found in the ocean. Arnosti et al. (2021) estimate that approximately half of the DOC reported by Hansell et al. (2009) can be attributed to the polysaccharide pool. As we focused our study on the the upper ocean biogeochemistry, we did not retrieve a total budget of dissolved or particulate organic carbon in the global ocean.

The definition of dissolved and particulate organic carbon is based on filtration (Repeta and Aluwihare, 2024). However, a part of DOC may quickly form gels or particles and

disintegrate again at some point (Arnosti et al., 2021; Chin et al., 1998; Passow, 2002). Further, the stickiness of PCHO and TEP may contribute to an aggregation of other particles/phytoplankton cells and increase the POC formation in this way (Passow, 2002). The buoyancy of TEP depends on the ballasting material which is incorporated in these aggregates, and as such, determines the rising or sinking speed in the water column (Engel et al., 2020). The concentrations of PCHO and TEP alone do not allow a robust assessment of their contribution to POC export.

In our study, we implemented the parametrization of Engel et al. (2004) into a global ocean biogeochemistry model for a first assessment of the implementation in the context of the surface Arctic Ocean. We limited our analysis to the upper ocean because an assessment of the carbon export would require the addition of a TEP sinking parametrization, which would involve ballasting, microbial/zooplankton grazing, and degradation processes. We acknowledged these short-comes in the Discussion Section 4.3.

However, our simulation reveals regionally diverging trends in TEP concentration over the analyzed period. In the Fram Strait, Barents Sea, and the Eurasian Basin, TEP concentrations mostly decline over time, while increases are observed in other parts of the Arctic Ocean, particularly in the Kara, Laptev, and Beaufort Seas. The increase in TEP concentrations is related to an increase in NPP with a coincident decrease in available nitrate concentration in the upper 30 m of the water column. This results in a stronger nutrient limitation of phytoplankton growth and leads to the exudation of organic carbon in accordance with the carbon overflow hypothesis (Engel et al., 2020). This effect could be even more important in a future Arctic Ocean, where the central basins might even experience a decrease in nitrate availability (Oziel et al., 2022), and where ocean warming has been suggested to increase the exudation of polysaccharides (Engel et al., 2011). To give an outlook: We are currently preparing a follow-up study on the trends of TEP concentrations until the end of the century in the context of Arctic Amplification. On the long term, possible changes in the phytoplankton community and differences in carbon exudation rates could play an important role besides the nutrient and temperature effects (Engel et al., 2017).

Comment 4

The results seem to be quite sensitive to limiter function (eqs. 5-6). Please briefly describe how the threshold 0.2 and 0.151 was determined and if they are spatially varying?

Response: Thank you for the comment. The limiter functions in REcoM3 depend on the intracellular nitrogen to carbon ratio (N:C ratio). These equations have been originally proposed by Geider et al. (1998) and modified for REcoM by Schourup-Kristensen et al. (2014). The thresholds have been proposed by Geider et al. (1998) based on phytoplankton growth experiments (mostly lab experiments mentioned by Geider et al. (1998)) and are not modified further in our model setup. These values are not spatially varying. We added this to the description of the implementation (L. 180):

> The thresholds have been proposed by Geider et al. (1998) based on phytoplankton growth experiments and are not modified further in our model setup. These values are not spatially varying in our setup.

Comment 5

As the authors stated, this is an important first step toward advancing the air-sea coupling (L39-41) in ESMs. Can you elaborate your plans in this direction? Is it feasible to simulate the marine TEP emissions? What would be the cloud feedback and radiation budget effect mentioned? Will it be similar to DMS (Schwinger et al., 2017 BG, https://doi.org/10.5194/bg-14-3633-2017)? Can the authors estimate the magnitude of this effect?

Response: Thank you for the comment. These two organic carbon compounds, PCHO and TEP, can serve as precursors and tracers for biogenic aerosols from the upper ocean that are crucial for mixed-phase cloud formation, ultimately affecting the Arctic radiation budget (Leck and Bigg, 2005a; Orellana et al., 2011; Park et al., 2019; van Pinxteren et al., 2022). The net cloud radiative effect depends on cloud microphysical properties such as the presence of liquid or ice phase, which is determined by the availability and type of cloud condensation nuclei or ice-nucleating particles (Shupe and Intrieri, 2004). However, uncertainties persist regarding the sign and magnitude of trends in cloud

characteristics and their role in the ongoing Arctic climate change (Block et al., 2020; Pithan and Mauritsen, 2014; Taylor et al., 2022; Vihma et al., 2016).

In certain circumstances, primary marine organic aerosols dominate over cloud condensation nuclei resulting from secondary aerosol formation within the atmosphere (Leck and Bigg, 2005b; Schmale et al., 2021). With the retreat of the sea ice and ocean warming, additional local sources of cloud condensation nuclei and ice-nucleating particles may occur. Consequently, temporal patterns may change (Schmale et al., 2021; Taylor et al., 2022). Biogenic ice-nucleating particles potentially originate from local features in open water areas like leads in the sea ice or ongoing melting cycles (Galgani et al., 2016; Hartmann et al., 2020; Irish et al., 2017; Zeppenfeld et al., 2019). Biologically active parts of the MIZ and aged melt ponds have, in particular, been found to contain efficient ice-nucleating substances (Zeppenfeld et al., 2019). Among many other – often analytically undetermined – organic compounds, aerosol particles in the Arctic may contain polysaccharides and proteinaceous material of marine origin. Both are known for their ice-nucleating activity (Hawkins and Russell, 2010; Irish et al., 2017; Karl et al., 2019; Leck et al., 2013; Orellana et al., 2021; Rad et al., 2018; Wilson et al., 2015).

PCHO, TEP, and other organic compounds can be transferred to the atmosphere from the ocean surface, through either the bursting of seawater bubbles entrained by waves or biologically produced bubbles (Aller et al., 2017; Bigg and Leck, 2008; Norris et al., 2011), thereby contributing to the formation of organic aerosol particles (Leck and Bigg, 2005a; Orellana et al., 2011; van Pinxteren et al., 2022). Recently, high TEP number concentrations and high TEP mass concentrations were reported in ambient marine aerosol particles, suggesting that these particles may account for more than half of the particulate organic aerosol mass (Aller et al., 2017; Orellana et al., 2011; van Pinxteren et al., 2022). Orellana et al. (2011) have also shown that TEP might originate from the surface water, but there are indications that TEP could also be formed directly within the atmosphere out of precursors (van Pinxteren et al., 2022).

In the accompanying research, Leon-Marcos et al. (2025) present an approach to simulate the transfer of marine biogenic aerosol precursors derived from the ocean biogeochemistry model output described in the present manuscript to the atmosphere based on the OCEANFILMS (Organic Compounds from Ecosystems to Aerosols: Natural Films and Interfaces via Langmuir Molecular Surfactants) parameterization by Burrows et al. (2016). As such, OCEANFILMS serves as an interface between the organic carbon simulated in

FESOM2.1-REcoM3 and the primary marine organic aerosols simulated in the aerosol-climate model. Leon-Marcos et al. (2025) adapt the OCEANFILMS scheme to compute three molecular groups out of the FESOM2.1-REcoM3 ocean surface concentration of organic carbon, in particular PCHO, dissolved combined amino acids, and polar lipids. The refractory DOC groups are neglected because of their low contribution to the marine organic aerosol mass fraction (Burrows et al., 2014; Leon-Marcos et al., 2025). The organic mass fraction is specific for each group and determines how much organics are emitted along sea salt emissions (Eq. 3 in Leon-Marcos et al., 2025).

As such, the organic mass fractions of the three molecular groups are set as ocean boundary conditions for the aerosol-climate model in a test run spanning ten years at a resolution of 1.9°×1.9°. The organic mass fraction of polar lipids is one to two orders of magnitude higher than PCHO and dissolved combined amino acids, and exhibits the strongest seasonal patterns. As a result, global primary marine organic aerosol emissions are also dominated by polar lipids (87.2%), with PCHO contributing 2.3% and dissolved combined amino acids 10.5%. Overall, the primary marine organic aerosol emission adds up to 13.6 $\mathrm{Tg\,year^{-1}}$. Regarding the Arctic, Leon-Marcos et al. (2025) find that the primary marine organic aerosol emissions are low compared to other regions. Still, the share of these emissions is especially high during phytoplankton blooms compared to the total aerosol emissions (Leon-Marcos et al., 2025). In a further study, Leon-Marcos et al. (2026) analyzed the trend of the FESOM2.1–REcoM3 simulation for the last decades and could show that the overall primary marine organic aerosols increased by approximately 12%.

Comment 6

Most (if not all) of the presented analysis are for surface processes. Are TEP and PCHO in the model only exist near the surface layers and none below? Is that why the spin up was so short and if they exist below the mixed layer, are they in sufficiently steady state? Some discussions or presentations of impacts on interior biogeochemistry (if any) would be appreciated.

Response: Thank you for the comment. Yes, the spin up time was short because we wanted to focus on the surface and upper ocean processes. Additionally, long spin ups are

costly in the current high resolution and not always possible. Since FSOM2.1–REcoM3 is generally well evaluated (Gürses et al., 2023), we considered a short spin up appropriate.

Regarding the depth distribution of TEP and PCHO, we added depth profiles of TEP concentration as Supplementary Fig. A7 (Fig. 8 in this document). We added a brief description of the depth profiles to the Discussion Section 4.3 (L. 592–603).

> Regarding the carbon export to the deep ocean in FESOM2.1–REcoM3, there are two detritus classes sinking with either increasing speed with depth (following Kriest and Oschlies, 2008) or constant, fast sinking mimicking zooplankton fecal pellets (Karakuş et al., 2021). Regarding TEP, no explicit sinking of TEP themselves has been implemented in the model. Still, the FESOM2.1–REcoM3 simulation contains a substantial decrease of TEP concentration with depth alongside the phytoplankton biomass decrease with depth (Supplementary Fig. A7). In the Arctic Ocean, the TEP concentration rapidly decrease to zero in the upper 40 m, whereas the averaged TEP concentration in the Northern and Southern Hemisphere decrease more slowly to zero over the upper 100 m. Generally, TEP themselves are less dense than seawater and often remain suspended near the surface or even become buoyant. Therefore, the direct contribution of TEP to net carbon export is limited and is not taken into account in our model run. However, TEP interact with denser particles forming TEP-rich aggregates, which can significantly contribute to the vertical transport of POC out of surface waters. Our model describes the primary mechanism driving this aggregation by increasing the particle stickiness depending on TEP concentration (Eq. 7). Hence, the role of TEP in driving sinking is included in our model run.

Minor comments

Comment 7

Fig3 caption: mention that this is from model simulation. Why not add observations here?

Response: Thank you for the comment. This figure is inspired by Nöthig et al. (2020), who compiled measurements of the Fram Strait and the Arctic Ocean spanning the years 1991 to 2015. In analogy to this, we presented our simulated dataset in a similar manner for a direct comparison. In Section 3.1 (Lines 281ff.), we stated this reference when presenting the TChla panel of this figure. In the Discussion Section 4.1 (Lines 405ff.), our compiled dataset is compared directly to Nöthig et al. (2020) and other studies. Our results are described and compared for the other variables in a similar way. As such, we thoroughly discuss this figure along available observations. Still, in our opinion, adding observations to this figure would decrease readability, especially as these observational datasets are often based on varying depth range, temporal averages etc. Regarding TEP concentration in comparison to observations, we were confronted with similar problems—that's why we had introduced Table 5 with re-calculations for every single *in situ* dataset.

Following your suggestion, we added the reference to the FESOM2.1–REcoM simulation and a reference of Nöthig et al. (2020) to this figure caption for clarification:

> Box plots comparing regional differences for simulated total Chlorophyll *a* (TChla, panel a), particulate organic carbon (POC, panel b), dissolved acidic polysaccharides (PCHO, panel c), and transparent exopolymer particles (TEP, panel d) in analogy to a compilation of observations by Nöthig et al. (2020). [...].

Comment 8

Fig3 caption: remove extra ')'

Response: Thank you for the comment. We removed the surplus bracket in the caption.

> East Siberian Shelves (E Sib., 40.9k)

Comment 9

L295: add space after period.

Response: Thank you for the comment. We added a space after period.

Comment 10

L306: describe SIC

Response: Thank you for the comment. We spelled out the abbreviation as this is the first use.

Comment 11

Fig4: why are there 'discontinuity' in the red lines?

Response: Thank you for the comment. We re-rendered the figure for continuous lines depicting the sea-ice edge and replaced the original one (Fig. 6/ Fig. 6 in this document).

Comment 12

Fig5: Any observations that can be plotted together (e.g. in same color dashed lines)?

Response: Thank you for the comment. This figure builds on the climatological monthly average of 2000 to 2019 as volume-weighted mean of the upper 30 m ocean depth of the simulated variables in FESOM2.1–REcoM3. As the Fram Strait, but also the entire Arctic Ocean, is a highly dynamical region, we need context for comparing the simulation to observations. For example, we discussed the TEP observations in comparison to our simulation extensively in the manuscript in Section 4.3, as additional details for each comparison were needed (time frame, depth range, averaging method etc). That's why we refrained from adding observations into this figure which would not fit entirely to the depicted simulated variables.

Comment 13

Why only eastern Fram Strait in Fig. 5, I would think showing the western Fram Strait or N. Barents Sea could be interesting, showing also the sea-ice concentrations.

Response: Thank you for the comment. We calculated the climatologies for the western Fram Strait and the Barents Sea as well for your comparison (Fig. 9 in this document). In our manuscript, we aimed at explaining the general seasonal cycle and interplay of the depicted variables in this figure. When comparing the seasonal cycles of the different regions, there is a general pattern of a strong seasonality driven by light and nutrients, though the timing and peak concentrations might vary across regions. Because of this, we refrained from including various seasonal cycles in the manuscript. Furthermore, the impact of the sea ice cover is also discussed shortly alongside Fig. 4 in the manuscript in Section 3.2.

Comment 14

L340: in the eastern Fram Strait(?)

Response: Thank you for the comment. We agree and apologize for the confusion. The maximum TEP concentration is simulated for the eastern Fram Strait. We changed the text accordingly (L. 362).

> Maximum simulated TEP concentrations reach nearly 190 µg C L^{-1} in the eastern Fram Strait.

Comment 15

L344: "It peaks at 150μg C L-1 in August and quickly declines thereafter", this is inconsistent with Fig. 5.

Response: Thank you for the comment. We totally agree and corrected the value and month in the new version of the manuscript (L. 366).

It peaks at approximately 200 µg C L^{-1} in July and quickly declines thereafter.

Comment 16

Table 5: Eurasian Basin (3e-51): is this a typo?

Response: Thank you for the comment. The calculated values are indeed wrong, we apologize. The correct TEP concentration averaged for 0–200 m depth in August 2001 is 1.9413 ±1.001 µg C L^{-1}. We corrected this in Tab. 5:

Eurasian Basin, 0–200 m, 1.9 ±1.0 µg C L^{-1} modeled TEP concentration

Comment 17

L429: remove ')'

Response: Thank you for the comment. We removed the surplus parenthesis.

Comment 18

L461-4: Vertical profiles comparing model and observations would be useful.

Response: Thank you for the comment. Unfortunately, the observational datasets contain averaged TEP counts or TEP concentration for the upper 200 m of the water column, with very limited total coverage. Out of this anecdotal evidence, we tried to discuss the depth distribution of TEP measurements compared to the simulation in words. A depth profile for TEP was added as Supplementary Fig. A7 (Fig. 8 in this document) and discussed in Section 4.3. Regarding TEP, no explicit sinking has been implemented in the model because of its positive buoyancy. We added particle stickiness due to TEP as a driving primary mechanism of aggregation and export of POC (see our response to Comment 6). The FESOM2.1–REcoM3 simulation contains a substantial

decrease of TEP concentration with depth alongside the phytoplankton biomass decrease with depth (Supplementary Fig. A7/ 8 in this document).

Comment 19

L471: at the beginning of

Response: Thank you for the comment. We rephrased the sentence following your suggestion.

> At the beginning of the year, TEP concentrations rise with the beginning of summer and decrease quickly in autumn.

Comment 20

L472: and decrease toward

Response: Thank you for the comment. We corrected the spelling.

> The highest concentrations are simulated along the coastline and with a decrease toward the central Arctic Ocean.

Comment 21

L481: A scatter plots of TEP vs TChla (from Fig. 4), including DIN values could support this statement.

Response: Thank you for the comment. We created a figure on the TChla concentration versus the TEP concentration for the Fram Strait (20°W-20°E; 75-82°N) fo May to July 2017 building on Fig. 4 as suggested (Fig. 10 in this document). TChla concentration ranges from 0 to 5.6 $\mathrm{mg\,m^{-3}}$ and the TEP concentration spans 0 to approximately 400 $\mathrm{\mu g\,C\,L^{-1}}$, where the highest values are found for low TChla concentration. There

is no obvious link between these variables. However, DIN concentration ranges from 0 to approximately 5 mmol m^{-3}, where DIN decrease with higher TChla or higher TEP concentrations. This figure supports our statement, that TChla alone is not a good predictor for TEP concentration, but also other biogeochemical variables like nutrient concentrations have to be considered.

Comment 22

L493-6: The statement gives the impression that the correlation of 0.71 considers the data from Caitlin Ice Base, when in fact data less than 1umol is excluded (Fig. A4 caption). Please rephrase.

Response: Thank you for the comment. We rephrased the paragraph to clarify which observations were included or excluded, along with the reasons for these decisions (L. 594).

Regarding the Arctic-wide occurrence of TEP, the available observations are very limited in space and time. Each measurement depends on a very local set of ecological conditions shaping sea ice concentration, nutrient availability, and phytoplankton blooms. These in situ observations are compared to monthly integrated simulation results for a small area enclosing the corresponding observation location in Tab. 5, complementary to the maps of simulated TEP concentration in Fig. 8. Overall, there is a fairly good agreement of the simulated TEP concentration to in situ observations (correlation coefficient of 0.71; $p = 0.11$, see also Supplementary Fig. A6) when the simulation also successfully models the phytoplankton blooms. However, the modeled TEP concentrations being often slightly higher and differing particularly in two cases which have been excluded from the correlation: Firstly, the Catlin Ice Base measurement in the Canadian Arctic Archipelago, where Wurl et al. (2011) obtained their measurements from an under-ice phytoplankton bloom, which resulted in very high production of TEP. Such an event is not reproducible by FESOM2.1–REcoM3 because ice-algae are not explicitly modeled, and light-through-ice transmission is not adequately represented. Secondly and similarly in the Central Arctic Ocean, Olli et al. (2007) conducted a drift experiment measuring TEP concentration in the pack ice. The authors found a uniform depth distribution

of TEP along the drift track, which could be supplied by the continuous primary production in the upper water column in open leads and melt ponds. However, there is nearly no TEP simulated in this area by FESOM2.1–REcoM3. The absence could originate from the missing under-ice or ice-algae production in the model, which have been part of other modeling approaches (e.g., Castellani et al., 2017).

Furthermore, we also modified the caption of the Supplementary Fig. A6:

Data points for TEP measurements at Catlin Ice Base (Wurl et al., 2011) and in the Eurasian Basin (Olli et al., 2007) have been excluded because the simulation was unable to capture the observed phytoplankton blooms.

Comment 23

L581: 10-150 is not 'agreeing well' with 0-39. Please rephrase.

Response: Thank you for the comment. We rephrased the part on the Southern Ocean in the manuscript and added the standard deviation for the measurements, which is rather large. The paragraph now reads (L.643):

In the Southern Ocean during the blooming period between December and March, simulated TEP concentrations increase to approximately 10–150 $\mu g\,C\,L^{-1}$. In the open waters of the Southern Ocean, observational studies report 0–39 $\mu g\,C\,L^{-1}$ with a large standard deviation of $\pm 117\,\mu g\,C\,L^{-1}$ (Engel et al., 2020; Wurl and Cunliffe, 2017), whereas in the coastal waters, even higher TEP concentrations are measured of approximately 200 $\mu g\,C\,L^{-1}$ in Bransfield Strait (Corzo et al., 2005 reviewed in Wurl and Cunliffe, 2017). The exact timing of measurements in relation to the state of phytoplankton blooms seems to be critical, as the standard deviation of the measured TEP concentration can be rather large and the authors link the TEP production primarily to phytoplankton production.

Modified/added figures

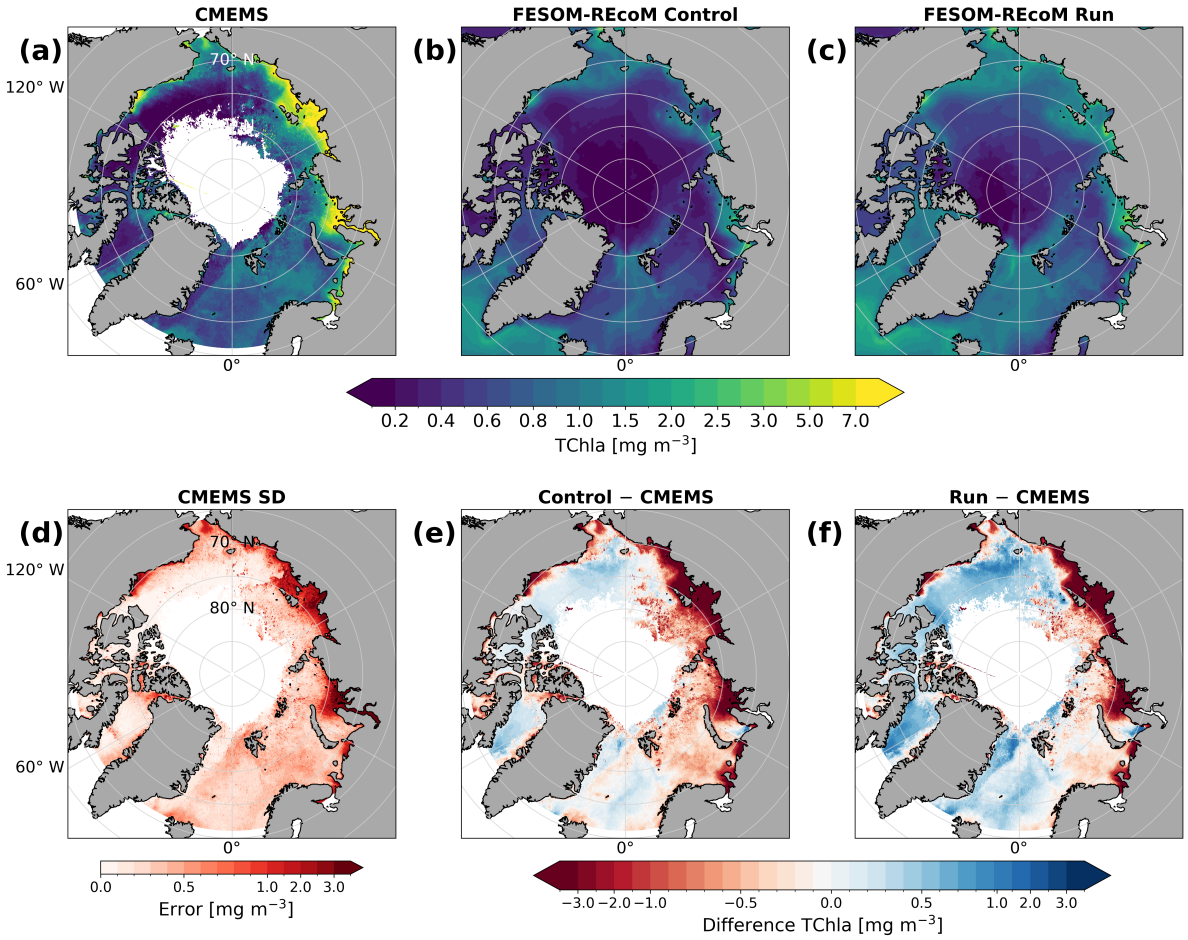

Figure 3: Maps of surface total Chlorophyll *a* (TChla) of Copernicus Marine Environment Monitoring Service level 4 monthly reprocessed Arctic Ocean Color product (CMEMS, panel a), of the FESOM2.1–REcoM3 control run without TEP (Control, panel b), of the FESOM2.1–REcoM3 run including transparent exopolymer particles (panel c), the standard deviation of TChla stated by CMEMS (SD, panel d), the difference of the control run compared to CMEMS (panel e), and the difference of the run including transparent exopolymer particles compared to CMEMS (panel f) as average of May to September of the years 2000 to 2019. CMEMS data does not cover the central Arctic Ocean.

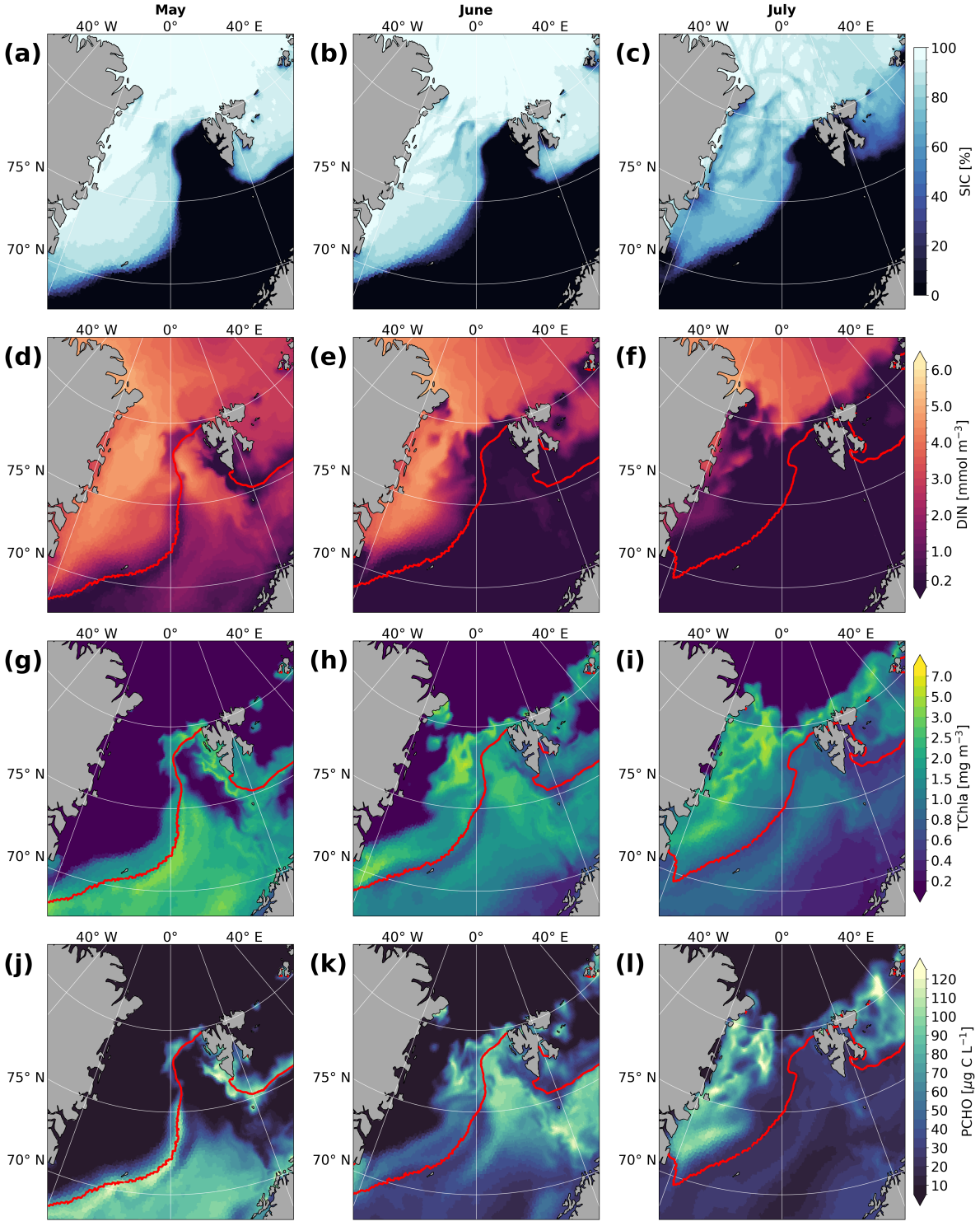

Figure 6: Maps of simulated sea-ice concentration (SIC, panel a–c), dissolved inorganic nitrogen (DIN, panel d–f), total Chlorophyll *a* (TChla, panel g–i) and dissolved acidic polysaccharides (PCHO, panel j–l) as monthly mean of May, June, and July 2017 for the model's surface layer (0–5 m). The contour of the sea-ice edge (defined as 25 % SIC) is depicted as red contour line.

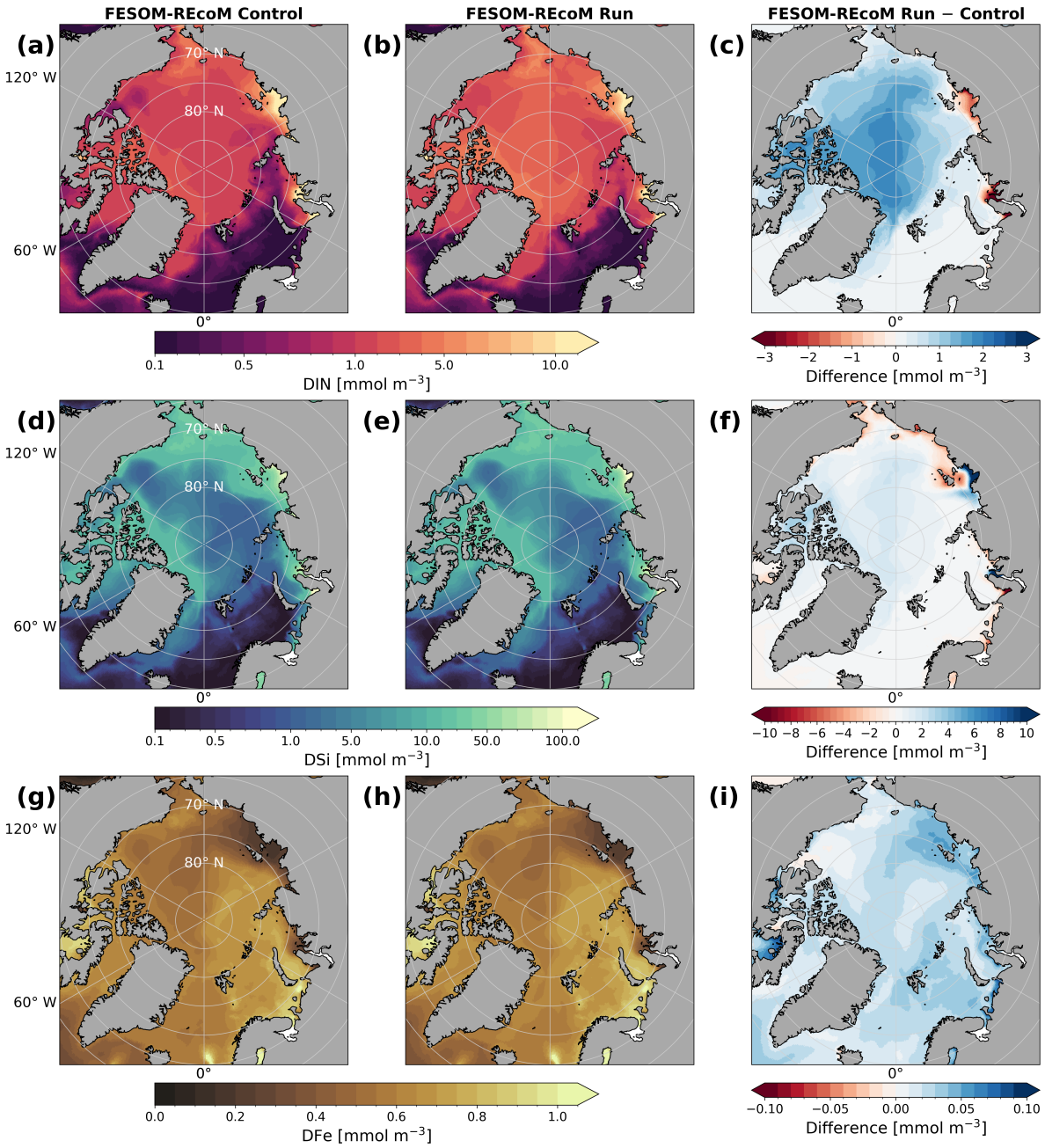

Figure 7: (Supplementary Fig. A3) Maps of volume-weighted main nutrient concentrations of the upper 30 m of the FESOM2.1–REcoM3 control run (first column) compared to the model run (second column), and their differences (third column). The panels depict dissolved inorganic nitrogen (first row, panel a-c), dissolved silicic acid (second row, panel d-f), and dissolved iron concentration (third row, panel g-i) as average of May to September of the years 2000 to 2019.

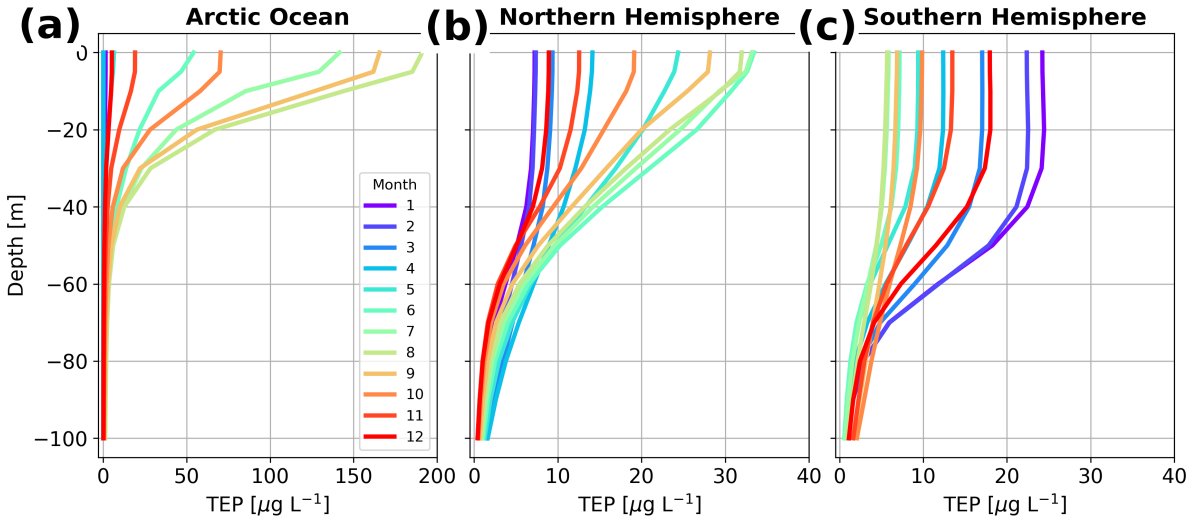

Figure 8: (Supplementary Fig. A7) Depth profiles of transparent exopolymer particle (TEP) concentration in the upper 100 m) as monthly mean of the years 2000 to 2019 for the Arctic Ocean (panel a), the northern hemisphere (panel b), and the southern hemisphere (panel c).

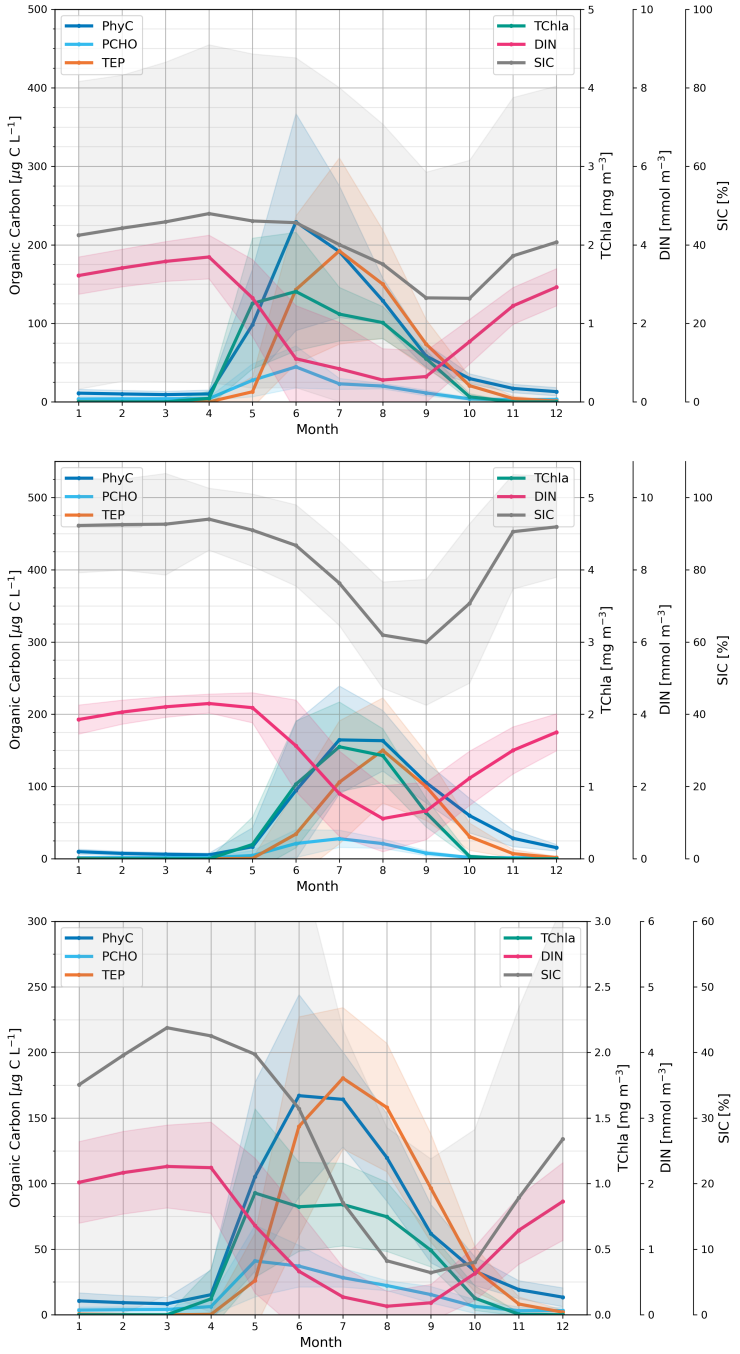

Figure 9: Climatologies for the eastern Fram Strait (upper panel), western Fram Strait (middle panel), and the Barents Sea (lower panel) Seasonal cycle of simulated organic carbon concentration of phytoplankton (PhyC, blue, sum of small phytoplankton and diatom carbon), dissolved acidic polysaccharides (PCHO, cyan), and transparent exopolymer particles (TEP, orange) on the left axis; as well as total Chlorophyll *a* (TChla, teal), dissolved inorganic nitrogen (DIN, magenta), and sea ice (SIC, grey) concentrations on the right axis of the period 2000 to 2019 as volume-weighted mean of the upper 30 m ocean depth, averaged each region, extent see Fig. 1). The standard deviation of each variable is computed from volume-weighted concentration across years and grid points in the regional subset and displayed as shaded area in corresponding colors.

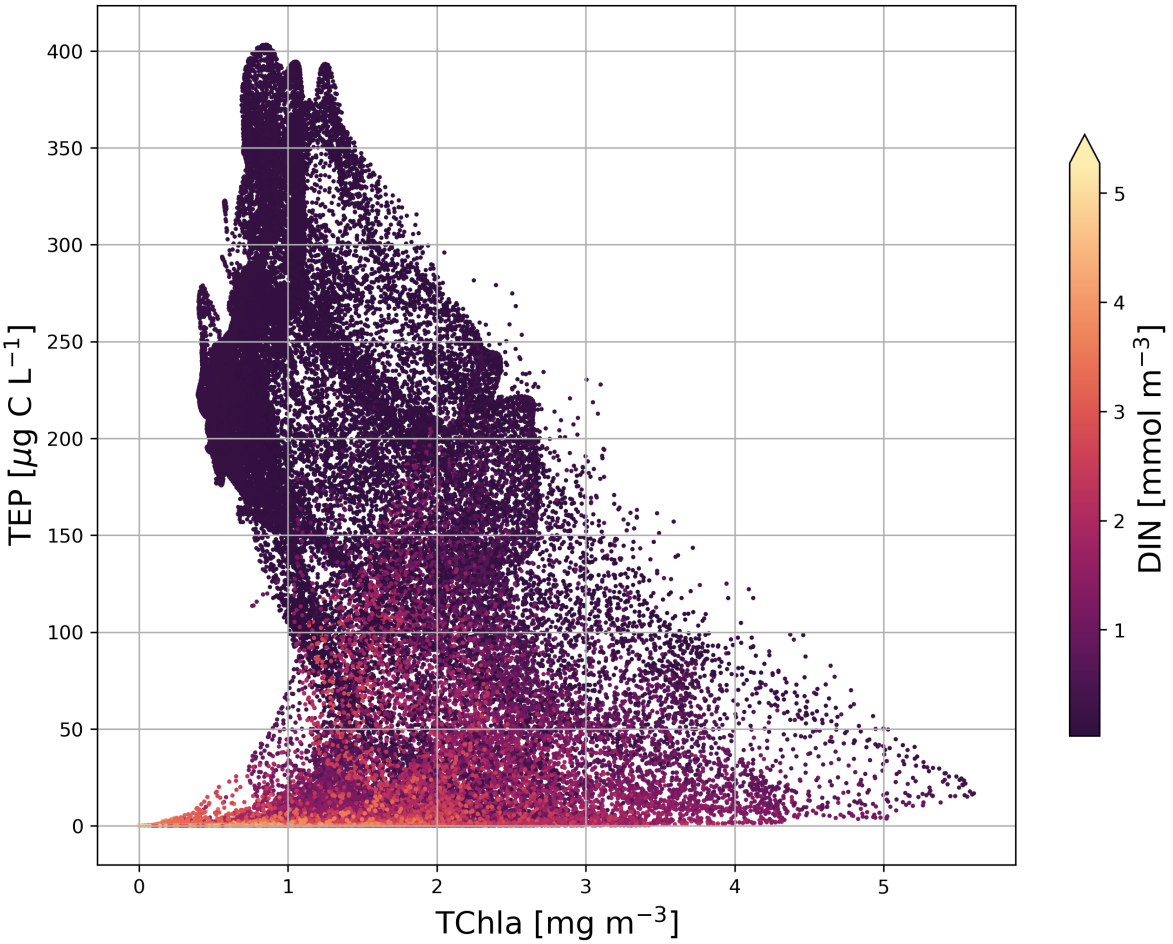

Figure 10: Scatter plot of Total Chlorophyll *a* vs. transparent exopolymer particle (TEP) ocean surface concentration in the Fram Strait (20°W-20°E; 75-82°N) of May to July 2017. This plot builds on Fig. 4 of the original manuscript, which depicts maps of ocean surface concentration in the Fram Strait for May, June, and July during the PASCAL campaign. The concentration of dissolved inorganic nitrogen (DIN) is coded as marker color.

Authors' Response to Reviewer 2

General Comments. The article "Assessment of transparent exopolymer particles in the Arctic Ocean implemented Into the coupled ocean–sea ice–biogeochemistry model FESOM2.1–REcoM3" by Zeising and colleagues presents new developments within the coupled physics-biogeochemistry model FESOM–REcoM allowing the simulation of PCHO and TEP, which are essential molecules produced by phytoplankton that have an increasingly recognized role in ocean particle dynamics and aerosol formation. This model is currently parametrized for Arctic ecosystems, but the authors provide a short global picture of TEP and PCHO.
This article is overall well written and the model evaluation is quite comprehensive and complete. The topic of the study is timely and the model developments presented here represent a promising avenue of research.
I have one major comment regarding the presentation of model results and more minor comments regarding model evaluation and the presentation of results.

Response: Thank you for your review of our manuscript. We appreciate all the constructive comments and suggestions, which we have carefully addressed in revising the manuscript. In the following, we provide detailed answers to the reviewer's comments and list the changes in the manuscript. We have carefully addressed all the issues item by item as follows.

Comment 1

The lack of a control simulation without PCHO and TEP production makes it difficult to assess the impacts of these tracers on ocean biogeochemistry.
If I understand correctly, the modeled PCHO is produced from phytoplankton exudation. Phytplankton exudation gives both DOC and PCHO. Is the total exudation (DOC+PCHO) different in this version of the model than in previous versions without PCHO? If yes: then I think the current model should be compared to a control simulation without PCHO exudation. If not, then maybe the model has already been evaluated previously and Chla should be the same as in previous versions? Then, I think model evaluation could be limited to PCHO and TEP data.

Response: Thank you for the comment. We agree that the manuscript can profit from a comparison to a control run. Therefore, we added the comparison to a control run without the implemented features conducted by us to several sections of the manuscript (see below). We also added a conceptual figure following your suggestion in Comment 6 to clarify the carbon cycle implemented in REcoM3.

Regarding your specific question on the exudation of DOC and PCHO: The total phytoplankton exudation is specified for small phytoplankton in Eq. 1. The exudation rate as such is determined by the phytoplankton carbon concentration, the exudation rate constant and the nutrient limitation. At this point, the phytoplankton exudation does not differ between DOC and PCHO. The organic carbon is just exuded by the phytoplankton. The equation is the same in both control without PCHO/TEP and model run containing PCHO/TEP. Only the next step, a difference between control and model run is introduced: In the control run, all of the exuded organic carbon is attributed to the DOC pool, whereas in the model run, the exuded organic carbon is split between the DOC and PCHO pool. In the model run, PCHO is described as a constant fraction of exuded organic carbon by the parameter f_{PCHO} in Eq. 3.

Comment 2

When evaluating model performances based on Chla concentrations (in sections 3.1 and 4.1), the model should be compared to satellite and to a control version.

Response: Thank you for the comment. We integrated a control run in our manuscript and enriched the evaluation as suggested in several parts of the manuscript. In the Methods, the control run is formally introduced (L. 117):

> Additionally, a FESOM2.1–REcoM3 control run was conducted using the same setup as described above but without the additional organic carbon process descriptions for PCHO and TEP.

For the general model assessment in terms of primary production, we added a comparison of the Total Chlorophyll *a* (TChla) concentrations of the simulation with the control run and the Copernicus remote-sensing data product to Fig. 3 (Fig. 3 in this document). In the Results Section, we added a figure description in Section 3.1 (L. 275–292):

The phytoplankton biomass in the surface Arctic Ocean in terms of TChla is depicted in Fig. 3, where the FESOM2.1–REcoM3 simulation is compared to the CMEMS Arctic satellite re-analysis product and a control run without TEP. The data is averaged over the years 2000 to 2019 (as a mean model state) for the months May to September when satellite data are available. The CMEMS TChla product shows no coverage of the central Arctic Ocean due to the satellite sensors configuration not enabling observations at these high latitudes (Fig. 3 panel a). In the Barents, Kara, and Laptev Seas, TChla ranges from 0.5 to 5 $\mathrm{mg\,m^{-3}}$, with peaks of up to 15 $\mathrm{mg\,m^{-3}}$ close to the coastline. In the East Siberian, Chukchi, and Beaufort Seas, the concentration of TChla is lower, ranging from 0.1 to 1 $\mathrm{mg\,m^{-3}}$, also with very high concentration close to the coast. The standard deviation of TChla from the CMEMS TChla product is mostly lower than 0.5 $\mathrm{mg\,m^{-3}}$. However, it increases to more than 2 $\mathrm{mg\,m^{-3}}$ along the coastline (Fig. 3 panel d). In the control simulation of FESOM2.1–REcoM3 without TEP, TChla concentration range from below 0.2 $\mathrm{mg\,m^{-3}}$ in the central Arctic Ocean to approximately 2 $\mathrm{mg\,m^{-3}}$ in the Fram Strait and Chukchi Sea, reaching even values of 3 $\mathrm{mg\,TChla\,m^{-3}}$ close to the coast of the Russian shelves. The FESOM2.1–REcoM3 including TEP simulates highest TChla concentrations of up to 6 $\mathrm{mg\,m^{-3}}$ along the Russian coast and in other shelf seas between 0.5 and 3 $\mathrm{mg\,m^{-3}}$ (Fig. 3 panel c). In the Fram Strait, TChla range from 1 to 3 $\mathrm{mg\,m^{-3}}$ with highest concentration in its central part, while in the central basins of the Arctic Ocean, TChla is generally low, with concentrations of up to 0.8 $\mathrm{mg\,m^{-3}}$. Compared to the control run without the TEP implementation, TChla concentrations are slightly elevated by 0.2 to 1 $\mathrm{mg\,m^{-3}}$ in the Fram Strait, in the Beaufort Gyre, and in the Chukchi Sea (Fig. 3 panel f). In the coastal areas of the Russian shelves, the simulated TChla is predominantly lower compared to the remote sensing product.

In the Discussion Section 4.1, we added more details on the TChla of the model run compared to the control run, to the CMEMS remote-sensing product, and to observations. We restructured and enriched the whole first part of the section (L. 404–453):

In terms of Arctic-wide TChla, the FESOM2.1–REcoM3 output is evaluated with the remote-sensing product provided by CMEMS and with various in situ datasets. Generally, FESOM2.1–REcoM3 aligns with the compiled remote-sensing data

of CMEMS TChla (Fig 3). The control run without the TEP implementation underestimates the TChla concentration in large parts of the Barents Sea and on the Arctic shelves, which was reported in Gürses et al. (2023) as well. Overall, the model run including TEP performs in better agreement with CMEMS. Still in the Chukchi Sea and the Beaufort Gyre, as well as in the Fram Strait, the model run overestimates the TChla compared to both the control run and CMEMS. Climatological monthly maps of TChla are included as Supplementary Fig. A2.
As such, this pattern of the FESOM2.1–REcoM3 model run compares well to the results from Nöthig et al. (2020) and also to other observations. The generally higher TChla concentrations in the model run compared to the control might reflect the higher turnover of phytoplankton biomass: TEP increases the aggregation of phytoplankton to detritus, which partly gets remineralized, replenishes nutrients to the seawater, and enables new build-up of phytoplankton biomass. In accordance with this hypothesis, we observe higher nutrient concentrations in the central Arctic Ocean, in the Beaufort Sea, and in the Chukchi Sea compared to the control run (Supplementary Fig. A3). However, we have not yet investigated the influence of TEP on the nutrient dynamics in the Arctic Ocean any further.
Evaluating the TChla patterns in more regional detail, we start with the eastern Fram Strait. Both CMEMS and the model run present the beginning of the phytoplankton bloom in May which prevails with TChla of approximately 1–3 $\mathrm{mgm^{-3}}$ through the summer months (Supplementary Fig. A4 and A2 panel a). In the eastern Fram Strait, in situ measurements of Nöthig et al. (2020) result in a median vertically integrated concentration of 44 $\mathrm{mg\,m^{-2}}$ (0–100 m depth), and in the Barents Sea of 42 $\mathrm{mg\,m^{-2}}$ which agree with simulated median concentrations of 40.4 and 33.8 $\mathrm{mg\,m^{-2}}$, respectively (Fig. 4 panel a). The results are also in line with the two-year round mooring observations at the long-term ecological research observatory HAUSGARTEN in the eastern Fram Strait with simulated TChla concentration reaching up to 5 $\mathrm{mg\,m^{-2}}$ in the upper 30 m compared to 7 $\mathrm{mg\,m^{-2}}$ in measurements (von Appen et al., 2021). In the MIZ, especially in the area of Fram Strait, phytoplankton growth is expected to be highest, as the sea-ice breaks up, light availability is increased and the water column is stratified (Cherkasheva et al., 2014; Nöthig et al., 2020). Likewise in the western part of Fram Strait and in the Siberian seas, the lower amount of simulated TChla matches in situ data for these regions spanning 13 to 26 $\mathrm{mg\,m^{-2}}$ (Nöthig et al., 2020; Piontek et al., 2021).

In the Chukchi and Beaufort Seas, the simulated TChla concentration itself (and the difference between FESOM2.1–REcoM3 and CMEMS) is generally low (less than 1.5 mg m^{-3}, Fig. 3 panel c and f). However, the timing of the phytoplankton bloom differs from May in CMEMS to June–July in the model run (Supplementary Fig. A4 and A2 panel a). Other observations from in situ data and satellite-derived products draw a diverse picture in these seas with massive under-ice blooms in the Chukchi Sea with high TChla concentration of up to 30 mg m^{-3} (Arrigo et al., 2014), and low (0.02–0.25 mg m^{-3}) TChla concentration in the northern Chukchi and Beaufort Seas (Jung et al., 2022; Park et al., 2019). In the central Arctic Ocean, vertically integrated TChla is low in both simulation (integrated over 0–100 m water depth, median 0.01 mg m^{-2}) and measurements (7–8 mg m^{-2}). No coverage by the remote-sensing product by CMEMS is available.

As such, the higher TChla concentration of the FESOM2.1–REcoM3 model run might be a better fit to observation data than CMEMS. One explanation for the observed difference may be that CMEMS sampled far less days than are simulated by FESOM2.1–REcoM3. Schourup-Kristensen et al. (2018) explain lower TChla in the simulation by full spatial and temporal coverage whereas only open-water productive regions are accessible from remote-sensing measurements. However, Assmy et al. (2017) suggest that remote-sensing products don't capture the phytoplankton bloom forming under thin ice or melt ponds, therefore often result in too low TChla estimates. A likely explanation for the higher simulated median TChla concentration in several regions and higher variability in comparison to Nöthig et al. (2020) might be the consideration of up to 62k data points in the regional subsets (Fig. 4 panel a) compared to only a few hundred in Nöthig et al. (2020), where the in situ sampling is mostly limited to one campaign each spring-summer season. Additionally, the evaluated regions of the model run contain the whole continental shelve grid points, whereas the in situ measurements are located mostly in the northern parts of the shelf seas (Nöthig et al., 2020).

However, in the coastal areas of the shelf areas (the Barents, Kara, and Laptev Seas and close to the Canadian coast) FESOM2.1–REcoM3 model run highly underestimates TChla concentrations provided by CMEMS (Fig. 3 panel c). There, CMEMS is error-prone (high standard deviation, Fig. 3 panel d), most likely due to the very high colored dissolved organic matter and total suspended matter concentrations, which have not been sufficiently accounted for in the retrieval

process. This results in a significant overestimation of TChla (Copernicus Marine Service, 2023; Heim et al., 2014; Schourup-Kristensen et al., 2018). Also other remote-sensing products overestimate TChla on the Arctic shelves (Mustapha et al., 2012).

Comment 3

In the results and discussion, the climatology of Chla is mentioned several times, I think that comparison of the climatology of Chla with satellite climatology would be strengthen your arguments.

Response: Thank you for the comment. We included the CMEMS climatology as monthly maps in the Supplement of the manuscript (Fig. A4/ Fig. 6 in this document) and used it for a comparison of TChla in the Discussion Section 4.1, which we restructured and cited in the reply to your comment above. However, the climatology of this remote-sensing product may as well exhibit the same uncertainties and overestimates of TChla especially on the shelves as discussed already in the manuscript. That's why we included also in situ datasets available for the assessment of TChla in the model run.

Minor comments

Comment 4

Intro lines 32-40: I am missing a little bit of numbers.
Maybe give some average concentrations of TEP measured? E.g. "remote marine regions, particularly the Arctic, organic compounds emitted from the upper ocean can serve as an important source of particles, thereby influencing the cloud feedback mechanisms and the overall radiation budget (Hamacher-Barth et al., 2016; Goosse et al., 2018; Hartmann et al., 2020; Ickes et al., 2020)." Is there an estimate of the flux or the proportion of organic compounds in the Arctic aerosols?

Response: Thank you for the comment. Because of the continuum of dissolved to particulate organic carbon, it is difficult to state the amount of PHCO and TEP present in the water column. Arnosti et al. (2021) estimate that approximately half of the amount of DOC calculated by Hansell et al. (2009) could be dissolved combined carbohydrates. In our introduction, we referenced these reviews among others. For TEP concentrations in the Arctic Ocean, there are measurements available which we had put into context in the Discussion section of our manuscript. Nevertheless, we added a sentence to the introduction following your recommendation (L. 36):

> For the Arctic Ocean, TEP concentrations of up to 405 µg C L^{-1} have been reported for the Canadian coast, and 7–139 µg C L^{-1} in the Fram Strait and on the shelves (Zamanillo et al., 2019).

Regarding the ocean-atmosphere interaction, we can refer to an accompanying research project. Leon-Marcos et al. (2025) present an approach to simulate the transfer of marine biogenic aerosol precursors derived from our model output to the atmosphere based on the OCEANFILMS (Organic Compounds from Ecosystems to Aerosols: Natural Films and Interfaces via Langmuir Molecular Surfactants) parameterization by Burrows et al. (2016). As such, OCEANFILMS serves as an interface between the organic carbon simulated in FESOM2.1-REcoM3 and the primary marine organic aerosols simulated in the aerosol-climate model.

As such, the organic mass fractions of the three molecular groups are set as ocean boundary conditions for the aerosol-climate model in a test run spanning ten years at a resolution of 1.9°×1.9°. As a result, global primary marine organic aerosol emissions are also dominated by polar lipids (87.2%), with PCHO contributing 2.3% and dissolved combined amino acids 10.5%. Overall, the primary marine organic aerosol emission adds up to 13.6 Tg $year^{-1}$. Regarding the Arctic, Leon-Marcos et al. (2025) find that the primary marine organic aerosol emissions are low compared to other regions. Still, the share of these emissions is especially high during phytoplankton blooms compared to the total aerosol emissions (Leon-Marcos et al., 2025).

Comment 5

You mention the PASCAL campaign several times, I think adding the location of the measurements on one of your maps would be good (e.g. On figure 1 or 4).

Response: Thank you for the comment. We understand your concern when trying to locate the campaign. However, the PASCAL measurements were compiled in categories for the open water, marginal ice zone, and pack ice. That's why there is no specific spot to mark on the maps in the figures suggested.

Comment 6

Paragraph lines 125-131: maybe add a simple schematics of the PCHO and TEP model?

Response: Thank you for the comment. We added a conceptional figure to the manuscript (Fig. 1/ Fig. 1 in this document) and linked the processes described in the lines 125-133 to it. The paragraph now reads (L. 129–137):

> In a first step, organic carbon is built up by photosynthesis in small phytoplankton and diatoms (Fig. 1, process A) and exuded in form of two different dissolved, labile pools: PCHO (B) and residual DOC (C, considered as consisting of labile organic compounds, but the chemical composition is not specified in greater detail). In a second step, multiple PCHO molecules may form aggregates or react with already existing TEP (D). Both DOC and TEP are remineralized to dissolved inorganic carbon (DIC, processes E and F). These processes are detailed out further below with respect to the simulated state equations. Following the organic carbon further, the phytoplankton classes are diminished by aggregation losses to detritus (G) and by grazing by the two zooplankton classes (H), where also the small zooplankton is grazed upon by macrozooplankton (I). Additionally, both zooplankton classes contribute to the detritus through sloppy feeding and mortality (J), but graze on these detritus particles as well (K). A surplus of organic carbon is excreted by zooplankton to DOC (L). Detritus particles can either degraded to DOC (M) or sink down into the water column (N), finally reaching the benthic layer.

Comment 7

Line 345 : you show the results of your simulations only for 0-30m, what do TEP and PCHO concentrations look like below ? Do they fall at 0 ?

Response: Thank you for the comment. We focused on the upper ocean because the implementation of TEP does not account for ballasting the sinking of ballasted TEP particles themselves. This model short-come was discussed in Section 4.3 (Lines 531-553). For clarification, we added a depth profile for TEP as Supplementary Fig. A7 (Fig. 8 in this document) and inserted a reference to it into the discussion in Section 4.3 (L. 594–598).

> Regarding TEP, no explicit sinking of TEP themselves has been implemented in the model because of its positive buoyancy. Still, the FESOM2.1–REcoM3 simulation contains a substantial decrease of TEP concentration with depth alongside the phytoplankton biomass decrease with depth (Supplementary Fig. A7). In the Arctic Ocean, the TEP concentration rapidly decrease to zero in the upper 40 m, whereas the averaged TEP concentration in the Northern and Southern Hemisphere decrease more slowly to zero over the upper 100 m.

Comment 8

Line 355 : you remind in this sentence that the model is optimized for the Arctic region, but also show global results. What are the implication of the Arctic parametrization on your global results ?

Response: Thank you for the comment. Our study builds on the tuning for the Arctic Ocean by Schourup-Kristensen et al. (2018) and Oziel et al. (2022), who focused on TChla and primary production in the tuning process. The Arctic-specific tuning involves parameterizations for aeolian and riverine nitrogen input, and benthic denitrification, which are not included in the global (standard) parametrization of REcoM3 by Gürses et al. (2023). Furthermore, we switched off the photo-damage parametrization implemented by Álvarez et al. (2019). This might lead to an increase of TChla concentrations in the global oceans compared to the standard parametrization. Additionally, we used the model grid

fARC providing a high resolution in the Arctic and a lower resolution elsewhere, which might result in weak upwelling or neglecting small-scale processes (Gürses et al., 2023).

There is no specific tuning for the implementation of PCHO and TEP for the Arctic Ocean. However, transferring the thoughts on TChla to the production of PCHO and TEP in the global ocean, we would expect that the tuning might as well result in higher PCHO and TEP concentrations (corresponding to the TChla concentration) compared to the standard setup.

Comment 9

Line 515 : "TEP aids in the aggregation of other particles (the TEP dependency of the aggregation rate, Eq. 7), but is not itself transferred in the process" even though TEP itself is not sinking, does it have an effect on particles sinking and subsequent C export in your model ? Since this is a potential strong implication of this work, I would like to see it discussed. Again, a comparison with a simulation without TEP would strengthen the demonstration.

Response: Thank you for the comment. The stickiness of PCHO and TEP may contribute to an aggregation of other particles/phytoplankton cells and increase the POC formation in this way (Passow, 2002). The buoyancy of TEP depends on the ballasting material which is incorporated in these aggregates, and as such, determines the rising or sinking speed in the water column (Engel et al., 2020). In our study, we implemented the parametrization of Engel et al. (2004) into a global ocean biogeochemistry model for a first assessment of the implementation in the context of the surface Arctic Ocean. We limited our analysis to the upper ocean because an assessment of the carbon export would require the addition of a TEP sinking parametrization, which would involve ballasting, microbial/zooplankton grazing, and degradation processes, which are not thoroughly investigated and quantified by observational data. We acknowledged these short-comes in the Discussion Section 4.3 and highlighted where observations and lab experiments could contribute to a more detailed parametrization in our model regarding carbon export.

So far, we included a first assessment on particulate organic carbon in our model run, which shapes the export of organic carbon. We presented the total concentration of POC integrated over the upper 100 m water column similar to the measurement compilation

of Nöthig et al. (2020) in our model run (Fig. 4) and compared it to this compilation region by region in the Discussion Section 4.1.

Following your suggestion, we added a figure displaying the impact of our implementation on the DOC and POC pools, which we included as maps for the whole Arctic Ocean as Fig. 5 (Fig. 5 in this document). We added a description of the control and model run regarding POC and DOC to the Results Section 3.1 (L. 299–304) and 3.2 (L. 323–326):

> Broadening the perspective from phytoplankton biomass to POC, the sum of the two phytoplankton, detritus and TEP (in the model run) pools is shown in Fig. 5. The simulated concentration reaches up to 400 µg C L^{-1} in the eastern Fram Strait and along the coastline of the shelves averaged over May to September of the upper 30 m (Fig. 5 panel b). In the central Arctic Ocean, the POC is mostly simulated with concentrations below 100 µg C L^{-1}. Thus, the model run results in POC concentrations of 100–200 µg C L^{-1} higher compared to the control, except for the central Arctic Ocean, where no large differences are found (Fig. 5 panel c).

> Comparing the dissolved part of organic carbon in FESOM2.1–REcoM3 between control run (without PCHO) and model run (with PCHO), both simulations result in highest DOC concentrations in the eastern Fram Strait and Barents Sea, with peaks along the coastline of the Russian shelves (Fig. 5 panel d and e). The DOC concentration in the control run spans approximately 100–150 µg C L^{-1}, where the DOC concentration in the model run ranges from 75 to 200 µg C L^{-1}.

The differences between the control and model run containing the PCHO and TEP implementation are now discussed in the Sections 4.2 for POC (L. 463–465, 476–480) and Section 4.3 for DOC (L. 517–528):

> The implementation of the additional processes for carbon exudation and aggregation impacts the amount and distribution of POC (Fig. 5). As such, the general agreement of simulated POC concentrations to observations confirms the improvement made in the model run.
> [...]
> Additionally, Engel et al. (2019) report 240 µg C L^{-1} POC in upper 30 m of the eastern Fram Strait in summer, which are comparable to the FESOM2.1–REcoM3

simulation of 200-350 µg C L^{-1} POC in the same area (Fig. 5 panel b). Further to the north of the Fram Strait, Gao et al. (2012) measured subsurface POC concentrations between 72 and 204 µg C L^{-1}, where the simulated POC concentration spans 50–100 µg C L^{-1}. The control run without the TEP implementation underestimates the POC concentration in all cases.

PCHO is considered a dissolved pool of organic carbon in FESOM2.1–REcoM3, which is generally part of the DOC pool when it comes to in situ methodology. However, we introduce a distinction between the DOC and the PCHO pool in the model setup, as the exuded phytoplankton organic carbon is split between DOC and PCHO. Furthermore, FESOM2.1–REcoM3 simulates only the (semi-)labile (fresh) DOC pool, which is considered as consisting of labile organic compounds and not refractory (old) ones. As such, a direct comparison of simulated DOC to observations results per se in the underestimation of DOC in the model. As such, in the Fram Strait, DOC concentrations of 720–2040 µg C L^{-1} have been reported for the upper 200 m of the water column (Engel et al., 2019, 2020; von Jackowski et al., 2020, 2022). von Jackowski et al. (2020) estimate the fraction of semi-labile DOC to 3.5–8.4 ±4.7% in their campaign, resulting in a concentration of 30–74 µg C L^{-1} semi-labile DOC. In the East Siberian Sea, DOC concentration reached 648 ±96 µg C L^{-1} during a bloom phytoplankton bloom (Jung et al., 2022). The FESOM2.1–REcoM3 model run yields higher DOC concentrations (sum of DOC and PCHO) compared to the control run (DOC, Fig. 5 panel f), with values still falling at the lower end of the in situ measurements cited above. Thus, we assume that the implementation of PCHO and TEP might result in a better fit to in situ measurements.

Modified/added figures

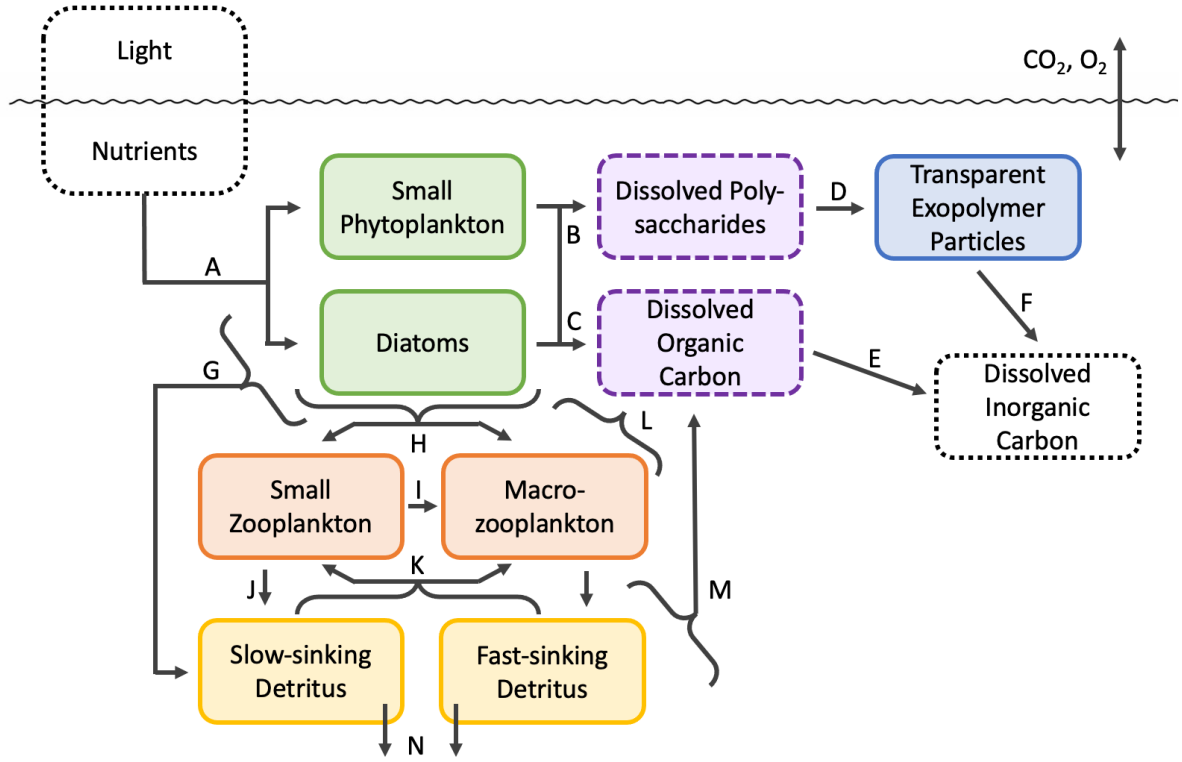

Figure 1: Concept of biogeochemistry processes included in the version of REcoM3 presented in this study. The labels refer to the processes described in Section 2.2.

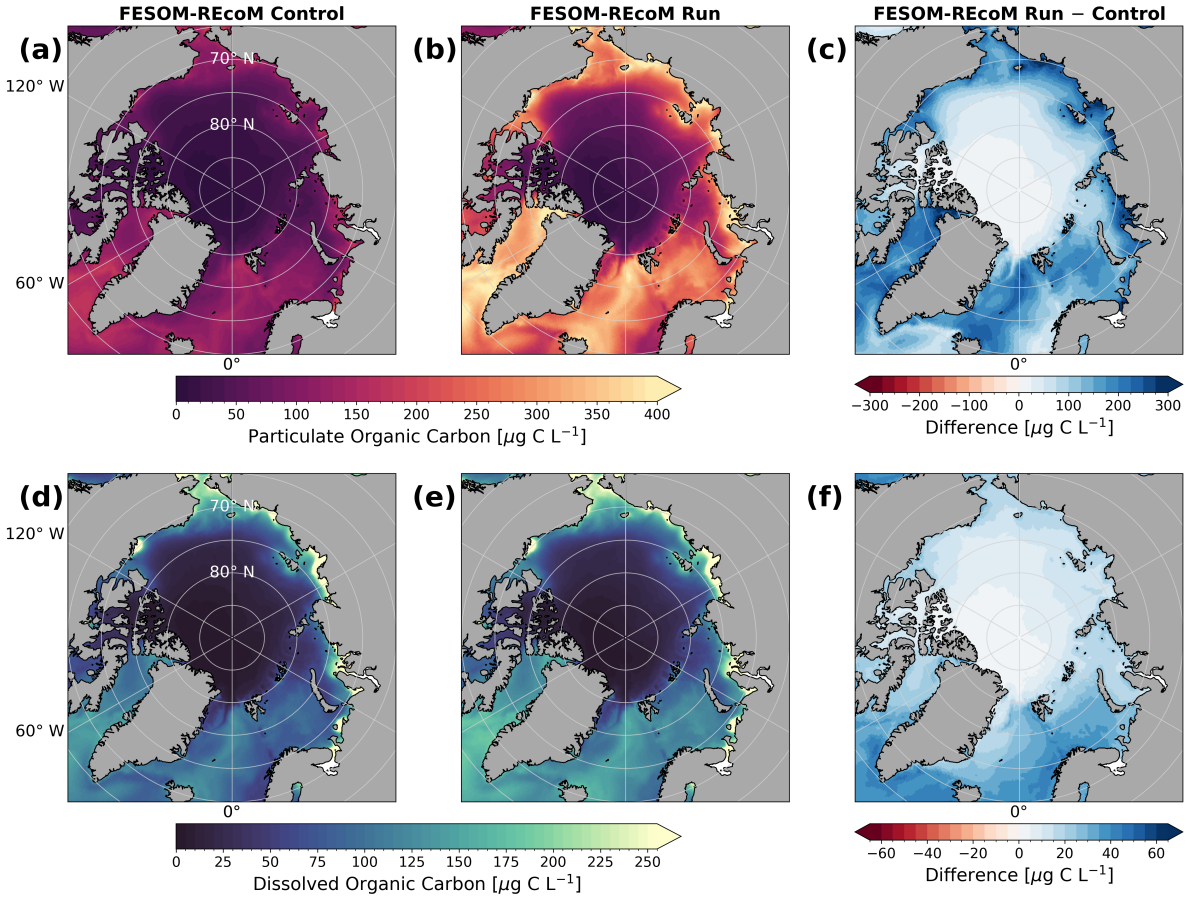

Figure 5: Maps of volume-weighted organic carbon concentrations of the upper 30 m of the FESOM2.1–REcoM3 control run (first column) compared to the model run (second column), and their differences (third column). The panels depict particulate organic carbon concentration as sum of diatoms, small phytoplankton, TEP and detritus (first row, panel a-c), and dissolved organic carbon (second row, panel d-f) as average of May to September of the years 2000 to 2019.

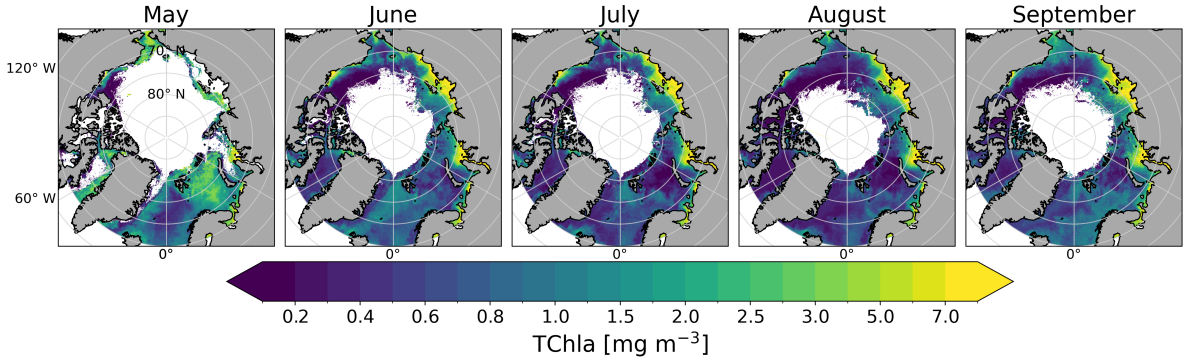

Figure 6: (Supplementary Fig. A4) Climatological maps of Copernicus Marine Environment Monitoring Service level 4 monthly reprocessed Arctic Ocean Color product (CMEMS) Total Chlorophyll *a* concentration of 2000 to 2019. CMEMS does not cover the central Arctic Ocean.

References

Aller, J. Y., Radway, J. C., Kilthau, W. P., Bothe, D. W., Wilson, T. W., Vaillancourt, R. D., Quinn, P. K., Coffman, D. J., Murray, B. J., and Knopf, D. A.: Size-Resolved Characterization of the Polysaccharidic and Proteinaceous Components of Sea Spray Aerosol, Atmospheric Environment, 154, 331–347, https://doi.org/10.1016/j.atmosenv.2017.01.053, 2017.

Álvarez, E., Thoms, S., Bracher, A., Liu, Y., and Völker, C.: Modeling Photoprotection at Global Scale: The Relative Role of Nonphotosynthetic Pigments, Physiological State, and Species Composition, Global Biogeochemical Cycles, 33, https://doi.org/10.1029/2018GB006101, 2019.

Arnosti, C., Wietz, M., Brinkhoff, T., Hehemann, J.-H., Probandt, D., Zeugner, L., and Amann, R.: The Biogeochemistry of Marine Polysaccharides: Sources, Inventories, and Bacterial Drivers of the Carbohydrate Cycle, Annual Review of Marine Science, 13, 81–108, https://doi.org/10.1146/annurev-marine-032020-012810, 2021.

Arrigo, K. R., Perovich, D. K., Pickart, R. S., Brown, Z. W., van Dijken, G. L., Lowry, K. E., Mills, M. M., Palmer, M. A., Balch, W. M., Bates, N. R., et al.: Phytoplankton Blooms beneath the Sea Ice in the Chukchi Sea, Deep Sea Research Part II: Topical Studies in Oceanography, 105, 1–16, 2014.

Assmy, P., Fernández-Méndez, M., Duarte, P., Meyer, A., Randelhoff, A., Mundy, C. J., Olsen, L. M., Kauko, H. M., Bailey, A., Chierici, M., et al.: Leads in Arctic Pack Ice Enable Early Phytoplankton Blooms below Snow-Covered Sea Ice, Scientific Reports, 7, 40 850, 2017.

Bigg, E. K. and Leck, C.: The Composition of Fragments of Bubbles Bursting at the Ocean Surface, Journal of Geophysical Research: Atmospheres, 113, 2008.

Block, K., Schneider, F. A., Mülmenstädt, J., Salzmann, M., and Quaas, J.: Climate Models Disagree on the Sign of Total Radiative Feedback in the Arctic, Tellus A: Dynamic Meteorology and Oceanography, 72, 1–14, https://doi.org/10.1080/16000870.2019.1696139, 2020.

Burrows, S. M., Ogunro, O., Frossard, A. A., Russell, L. M., Rasch, P. J., and Elliott, S. M.: A Physically Based Framework for Modeling the Organic Fractionation of Sea Spray Aerosol from Bubble Film Langmuir Equilibria, Atmos. Chem. Phys., 14, 13 601–13 629, https://doi.org/10.5194/acp-14-13601-2014, 2014.

Burrows, S. M., Gobrogge, E., Fu, L., Link, K., Elliott, S. M., Wang, H., and Walker, R.: OCEANFILMS-2: Representing Coadsorption of Saccharides in Marine Films and Potential

Impacts on Modeled Marine Aerosol Chemistry, Geophysical Research Letters, 43, 8306–8313, https://doi.org/10.1002/2016GL069070, 2016.

Castellani, G., Losch, M., Lange, B. A., and Flores, H.: Modeling Arctic Sea-Ice Algae: Physical Drivers of Spatial Distribution and Algae Phenology, Journal of Geophysical Research: Oceans, 122, 7466–7487, https://doi.org/10.1002/2017JC012828, 2017.

Cherkasheva, A., Bracher, A., Melsheimer, C., Köberle, C., Gerdes, R., Nöthig, E.-M., Bauerfeind, E., and Boetius, A.: Influence of the Physical Environment on Polar Phytoplankton Blooms: A Case Study in the Fram Strait, Journal of Marine Systems, 132, 196–207, https://doi.org/10.1016/j.jmarsys.2013.11.008, 2014.

Chin, W.-C., Orellana, M. V., and Verdugo, P.: Spontaneous Assembly of Marine Dissolved Organic Matter into Polymer Gels, Nature, 391, 568–572, https://doi.org/10.1038/35345, 1998.

Copernicus Marine Service: Quality Information Document, Tech. rep., Mercator Ocean International, 2023.

Corzo, A., Rodríguez-Gálvez, S., Lubian, L., Sangrá, P., Martínez, A., and Morillo, J. A.: Spatial Distribution of Transparent Exopolymer Particles in the Bransfield Strait, Antarctica, Journal of Plankton Research, 27, 635–646, https://doi.org/10.1093/plankt/fbi038, 2005.

Engel, A., Thoms, S., Riebesell, U., Rochelle-Newall, E., and Zondervan, I.: Polysaccharide Aggregation as a Potential Sink of Marine Dissolved Organic Carbon, Nature, 428, 929–932, https://doi.org/10.1038/nature02453, 2004.

Engel, A., Händel, N., Wohlers, J., Lunau, M., Grossart, H.-P., Sommer, U., and Riebesell, U.: Effects of Sea Surface Warming on the Production and Composition of Dissolved Organic Matter during Phytoplankton Blooms: Results from a Mesocosm Study, Journal of Plankton Research, 33, 357–372, https://doi.org/10.1093/plankt/fbq122, 2011.

Engel, A., Piontek, J., Metfies, K., Endres, S., Sprong, P., Peeken, I., Gäbler-Schwarz, S., and Nöthig, E.-M.: Inter-Annual Variability of Transparent Exopolymer Particles in the Arctic Ocean Reveals High Sensitivity to Ecosystem Changes, Scientific reports, 7, 1–9, 2017.

Engel, A., Bracher, A., Dinter, T., Endres, S., Grosse, J., Metfies, K., Peeken, I., Piontek, J., Salter, I., and Nöthig, E.-M.: Inter-Annual Variability of Organic Carbon Concentrations across the Fram Strait (Arctic Ocean) during Summer 2009–2017, Front. Mar. Sci., 6 (187), https://doi.org/doi:10.3389/fmars.2019.00187, 2019.

Engel, A., Endres, S., Galgani, L., and Schartau, M.: Marvelous Marine Microgels: On the Distribution and Impact of Gel-Like Particles in the Oceanic Water-Column, Frontiers in Marine Science, 7, 405, https://doi.org/10.3389/fmars.2020.00405, 2020.

Galgani, L., Piontek, J., and Engel, A.: Biopolymers Form a Gelatinous Microlayer at the Air-Sea Interface When Arctic Sea Ice Melts, Scientific Reports, 6, 29 465, https://doi.org/10.1038/srep29465, 2016.

Gao, Q., Leck, C., Rauschenberg, C., and Matrai, P. A.: On the Chemical Dynamics of Extracellular Polysaccharides in the High Arctic Surface Microlayer, Ocean Sci., 8, 401–418, https://doi.org/10.5194/os-8-401-2012, 2012.

Garcia, HE., Weathers, KW., Paver, CR., Smolyar, I., Boyer, TP., Locarnini, MM., Zweng, MM., Mishonov, AV., Baranova, OK., and Seidov, D.: World Ocean Atlas 2018, Volume 3: Dissolved Oxygen, Apparent Oxygen Utilization, and Dissolved Oxygen Saturation., A. Mishonov Technical Editor, Tech. rep., NOAA Atlas NESDIS, 2019a.

Garcia, HE., Weathers, KW., Paver, CR., Smolyar, I., Boyer, TP., Locarnini, MM., Zweng, MM., Mishonov, AV., Baranova, OK., and Seidov, D.: World Ocean Atlas 2018. Vol. 4: Dissolved Inorganic Nutrients (Phosphate, Nitrate and Nitrate+ Nitrite, Silicate), A. Mishonov Technical Editor, Tech. rep., NOAA Atlas NESDIS, 2019b.

Geider, R. J., Maclntyre, H. L., and Kana, T. M.: A Dynamic Regulatory Model of Phytoplanktonic Acclimation to Light, Nutrients, and Temperature, Limnology and Oceanography, 43, 679–694, https://doi.org/10.4319/lo.1998.43.4.0679, 1998.

Gürses, Ö., Oziel, L., Karakuş, O., Sidorenko, D., Völker, C., Ye, Y., Zeising, M., Butzin, M., and Hauck, J.: Ocean Biogeochemistry in the Coupled Ocean–Sea Ice–Biogeochemistry Model FESOM2.1–REcoM3, Geosci. Model Dev., 16, 4883–4936, https://doi.org/10.5194/gmd-16-4883-2023, 2023.

Hansell, D., Carlson, C., Repeta, D., and Schlitzer, R.: Dissolved Organic Matter in the Ocean: A Controversy Stimulates New Insights, Oceanography, 22, 202–211, https://doi.org/10.5670/oceanog.2009.109, 2009.

Hartmann, M., Adachi, K., Eppers, O., Haas, C., Herber, A., Holzinger, R., Hünerbein, A., Jäkel, E., Jentzsch, C., van Pinxteren, M., Wex, H., Willmes, S., and Stratmann, F.: Wintertime Airborne Measurements of Ice Nucleating Particles in the High Arctic: A Hint to a Marine, Biogenic Source for Ice Nucleating Particles, Geophysical Research Letters, 47, e2020GL087 770, https://doi.org/10.1029/2020GL087770, 2020.

Hawkins, L. N. and Russell, L. M.: Polysaccharides, Proteins, and Phytoplankton Fragments: Four Chemically Distinct Types of Marine Primary Organic Aerosol Classified by Single Particle Spectromicroscopy, Advances in Meteorology, 2010, 612 132–, https://doi.org/10.1155/2010/612132, 2010.

Heim, B., Abramova, E., Doerffer, R., Günther, F., Hölemann, J., Kraberg, A., Lantuit, H., Loginova, A., Martynov, F., Overduin, P. P., and Wegner, C.: Ocean Colour Remote Sensing in the Southern Laptev Sea: Evaluation and Applications, Biogeosciences, 11, 4191–4210, https://doi.org/10.5194/bg-11-4191-2014, 2014.

Irish, V. E., Elizondo, P., Chen, J., Chou, C., Charette, J., Lizotte, M., Ladino, L. A., Wilson, T. W., Gosselin, M., Murray, B. J., Polishchuk, E., Abbatt, J. P. D., Miller, L. A., and Bertram, A. K.: Ice-Nucleating Particles in Canadian Arctic Sea-Surface Microlayer and Bulk Seawater, Atmospheric Chemistry and Physics, 17, 10 583–10 595, https://doi.org/10.5194/acp-17-10583-2017, 2017.

Jung, J., Lee, Y., Cho, K.-H., Yang, E. J., and Kang, S.-H.: Spatial Distributions of Riverine and Marine Dissolved Organic Carbon in the Western Arctic Ocean: Results From the 2018 Korean Expedition, Journal of Geophysical Research: Oceans, 127, e2021JC017 718, https://doi.org/10.1029/2021JC017718, 2022.

Karakuş, O., Völker, C., Iversen, M., Hagen, W., Gladrow, D. W., Fach, B., and Hauck, J.: Modeling the Impact of Macrozooplankton on Carbon Export Production in the Southern Ocean, Journal of Geophysical Research: Oceans, n/a, e2021JC017 315, https://doi.org/10.1029/2021JC017315, 2021.

Karl, M., Leck, C., Mashayekhy Rad, F., Bäcklund, A., Lopez-Aparicio, S., and Heintzenberg, J.: New Insights in Sources of the Sub-Micrometre Aerosol at Mt. Zeppelin Observatory (Spitsbergen) in the Year 2015, Tellus B: Chemical and Physical Meteorology, 71, 1613 143, https://doi.org/10.1080/16000889.2019.1613143, 2019.

Kriest, I. and Oschlies, A.: On the Treatment of Particulate Organic Matter Sinking in Large-Scale Models of Marine Biogeochemical Cycles, Biogeosciences, 5, 55–72, https://doi.org/10.5194/bg-5-55-2008, 2008.

Leck, C. and Bigg, E. K.: Biogenic Particles in the Surface Microlayer and Overlaying Atmosphere in the Central Arctic Ocean during Summer, Tellus B: Chemical and Physical Meteorology, 57, 305–316, https://doi.org/10.3402/tellusb.v57i4.16546, 2005a.

Leck, C. and Bigg, E. K.: Source and Evolution of the Marine Aerosol—A New Perspective, Geophysical Research Letters, 32, https://doi.org/10.1029/2005GL023651, 2005b.

Leck, C., Gao, Q., Mashayekhy Rad, F., and Nilsson, U.: Size-Resolved Atmospheric Particulate Polysaccharides in the High Summer Arctic, Atmospheric Chemistry and Physics, 13, 12 573–12 588, https://doi.org/10.5194/acp-13-12573-2013, 2013.

Leon-Marcos, A., Zeising, M., van Pinxteren, M., Zeppenfeld, S., Bracher, A., Barbaro, E., Engel, A., Feltracco, M., Tegen, I., and Heinold, B.: Modelling Emission and Transport of Key Components of Primary Marine Organic Aerosol Using the Global Aerosol–Climate Model ECHAM6.3–HAM2.3, Geosci. Model Dev., 18, 4183–4213, https://doi.org/10.5194/gmd-18-4183-2025, 2025.

Leon-Marcos, A., van Pinxteren, M., Zeppenfeld, S., Zeising, M., Bracher, A., Oziel, L., Tegen, I., and Heinold, B.: Thirty years of arctic primary marine organic aerosols: patterns, seasonal dynamics, and trends (1990–2019), 26, 1109–1144, https://doi.org/10.5194/acp-26-1109-2026, 2026.

Mustapha, S. B., , Simon, B., and and Larouche, P.: Evaluation of Ocean Color Algorithms in the Southeastern Beaufort Sea, Canadian Arctic: New Parameterization Using SeaWiFS, MODIS, and MERIS Spectral Bands, Canadian Journal of Remote Sensing, 38, 535–556, https://doi.org/10.5589/m12-045, 2012.

Norris, S. J., Brooks, I. M., de Leeuw, G., Sirevaag, A., Leck, C., Brooks, B. J., Birch, C. E., and Tjernström, M.: Measurements of Bubble Size Spectra within Leads in the Arctic Summer Pack Ice, Ocean Sci., 7, 129–139, https://doi.org/10.5194/os-7-129-2011, 2011.

Nöthig, E.-M., Ramondenc, S., Haas, A., Hehemann, L., Walter, A., Bracher, A., Lalande, C., Metfies, K., Peeken, I., Bauerfeind, E., and Boetius, A.: Summertime Chlorophyll a and Particulate Organic Carbon Standing Stocks in Surface Waters of the Fram Strait and the Arctic Ocean (1991–2015), Frontiers in Marine Science, 7, 350, https://doi.org/10.3389/fmars.2020.00350, 2020.

Olli, K., Wassmann, P., Reigstad, M., Ratkova, T. N., Arashkevich, E., Pasternak, A., Matrai, P. A., Knulst, J., Tranvik, L., Klais, R., and Jacobsen, A.: The Fate of Production in the Central Arctic Ocean – Top–down Regulation by Zooplankton Expatriates?, Progress in Oceanography, 72, 84–113, https://doi.org/10.1016/j.pocean.2006.08.002, 2007.

Orellana, M. V., Matrai, P. A., Leck, C., Rauschenberg, C. D., Lee, A. M., and Coz, E.: Marine Microgels as a Source of Cloud Condensation Nuclei in the High Arctic, Proc. Natl. Acad. Sci., 108, 13 612–13 617, https://doi.org/10.1073/pnas.1102457108, 2011.

Orellana, M. V., Hansell, D. A., Matrai, P. A., and Leck, C.: Marine Polymer-Gels' Relevance in the Atmosphere as Aerosols and CCN, Gels, 7, https://doi.org/10.3390/gels7040185, 2021.

Oziel, L., Schourup-Kristensen, V., Wekerle, C., and Hauck, J.: The Pan-Arctic Continental Slope as an Intensifying Conveyer Belt for Nutrients in the Central Arctic Ocean (1985–2015), Global Biogeochemical Cycles, 36, e2021GB007 268, https://doi.org/10.1029/2021GB007268, 2022.

Park, J., Dall'Osto, M., Park, K., Kim, J.-H., Park, J., Park, K.-T., Hwang, C. Y., Jang, G. I., Gim, Y., Kang, S., Park, S., Jin, Y. K., Yum, S. S., Simó, R., and Yoon, Y. J.: Arctic Primary Aerosol Production Strongly Influenced by Riverine Organic Matter, Environmental Science & Technology, 53, 8621–8630, https://doi.org/10.1021/acs.est.9b03399, 2019.

Passow, U.: Transparent Exopolymer Particles (TEP) in Aquatic Environments, Progress in Oceanography, 55, 287–333, https://doi.org/10.1016/S0079-6611(02)00138-6, 2002.

Piontek, J., Galgani, L., Nöthig, E.-M., Peeken, I., and Engel, A.: Organic Matter Composition and Heterotrophic Bacterial Activity at Declining Summer Sea Ice in the Central Arctic Ocean, Limnology and Oceanography, 66, S343–S362, https://doi.org/10.1002/lno.11639, 2021.

Pithan, F. and Mauritsen, T.: Arctic Amplification Dominated by Temperature Feedbacks in Contemporary Climate Models, Nature Geoscience, 7, 181–184, https://doi.org/10.1038/ngeo2071, 2014.

Rad, F. M., Zurita, J., Gilles, P., Rutgeerts, L. A. J., Nilsson, U., Ilag, L. L., and Leck, C.: Measurements of Atmospheric Proteinaceous Aerosol in the Arctic Using a Selective UHPLC/ESI-MS/MS Strategy, Journal of the American Society for Mass Spectrometry, 30, 161–173, https://doi.org/10.1007/s13361-018-2009-8, 2018.

Repeta, D. and Aluwihare, L.: Chemical Characterization and Cycling of Dissolved Organic Matter, in: Biogeochemistry of Marine Dissolved Organic Matter, pp. 13–67, Elsevier, ISBN 978-0-443-13858-4, https://doi.org/10.1016/B978-0-443-13858-4.00011-3, 2024.

Schmale, J., Zieger, P., and Ekman, A. M. L.: Aerosols in Current and Future Arctic Climate, Nature Climate Change, 11, 95–105, https://doi.org/10.1038/s41558-020-00969-5, 2021.

Schourup-Kristensen, V., Sidorenko, D., Wolf-Gladrow, D. A., and Völker, C.: A Skill Assessment of the Biogeochemical Model REcoM2 Coupled to the Finite Element Sea Ice–Ocean Model (FESOM 1.3), Geoscientific Model Development, 7, 2769–2802, https://doi.org/10.5194/gmd-7-2769-2014, 2014.

Schourup-Kristensen, V., Wekerle, C., Wolf-Gladrow, D. A., and Völker, C.: Arctic Ocean Biogeochemistry in the High Resolution FESOM 1.4-REcoM2 Model, Progress in Oceanography, 168, 65–81, https://doi.org/10.1016/j.pocean.2018.09.006, 2018.

Shupe, M. D. and Intrieri, J. M.: Cloud Radiative Forcing of the Arctic Surface: The Influence of Cloud Properties, Surface Albedo, and Solar Zenith Angle, Journal of Climate, 17, 616–628, https://doi.org/10.1175/1520-0442(2004)017<0616:CRFOTA>2.0.CO;2, 2004.

Taylor, P. C., Boeke, R. C., Boisvert, L. N., Feldl, N., Henry, M., Huang, Y., Langen, P. L., Liu, W., Pithan, F., Sejas, S. A., and Tan, I.: Process Drivers, Inter-Model Spread, and the Path Forward: A Review of Amplified Arctic Warming, Frontiers in Earth Science, 9, https://doi.org/10.3389/feart.2021.758361, 2022.

van Pinxteren, M., Robinson, T.-B., Zeppenfeld, S., Gong, X., Bahlmann, E., Fomba, K. W., Triesch, N., Stratmann, F., Wurl, O., Engel, A., Wex, H., and Herrmann, H.: High Number Concentrations of Transparent Exopolymer Particles in Ambient Aerosol Particles and Cloud Water – a Case Study at the Tropical Atlantic Ocean, Atmos. Chem. Phys., 22, 5725–5742, https://doi.org/10.5194/acp-22-5725-2022, 2022.

Vihma, T., Screen, J., Tjernström, M., Newton, B., Zhang, X., Popova, V., Deser, C., Holland, M., and Prowse, T.: The Atmospheric Role in the Arctic Water Cycle: A Review on Processes, Past and Future Changes, and Their Impacts, Journal of Geophysical Research: Biogeosciences, 121, 586–620, https://doi.org/10.1002/2015JG003132, 2016.

von Appen, W.-J., Waite, A. M., Bergmann, M., Bienhold, C., Boebel, O., Bracher, A., Cisewski, B., Hagemann, J., Hoppema, M., Iversen, M. H., Konrad, C., Krumpen, T., Lochthofen, N., Metfies, K., Niehoff, B., Nöthig, E.-M., Purser, A., Salter, I., Schaber, M., Scholz, D., Soltwedel, T., Torres-Valdes, S., Wekerle, C., Wenzhöfer, F., Wietz, M., and Boetius, A.: Sea-Ice Derived Meltwater Stratification Slows the Biological Carbon Pump: Results from Continuous Observations, Nature Communications, 12, 7309, https://doi.org/10.1038/s41467-021-26943-z, 2021.

von Jackowski, A., Grosse, J., Nöthig, E.-M., and Engel, A.: Dynamics of Organic Matter and Bacterial Activity in the Fram Strait during Summer and Autumn, Philosophical Transactions of the Royal Society A: Mathematical, Physical and Engineering Sciences, 378, 20190 366, https://doi.org/10.1098/rsta.2019.0366, 2020.

von Jackowski, A., Becker, K. W., Wietz, M., Bienhold, C., Zäncker, B., Nöthig, E.-M., and Engel, A.: Variations of Microbial Communities and Substrate Regimes in the Eastern Fram Strait between Summer and Fall, Environmental Microbiology, n/a, https://doi.org/10.1111/1462-2920.16036, 2022.

Wilson, T. W., Ladino, L. A., Alpert, P. A., Breckels, M. N., Brooks, I. M., Browse, J., Burrows, S. M., Carslaw, K. S., Huffman, J. A., Judd, C., et al.: A Marine Biogenic

Source of Atmospheric Ice-Nucleating Particles, Nature, 525, 234–238, https://doi.org/10.1038/nature14986, 2015.

Wurl, O. and Cunliffe, M.: Transparent Exopolymeric Particles: An Important EPS Component in Seawater, in: The Perfect Slime: Microbial Extracellular Polymeric Substances (EPS), pp. 249–267, IWA publishing, London, ISBN 1-78040-741-6, 2017.

Wurl, O., Miller, L., and Vagle, S.: Production and Fate of Transparent Exopolymer Particles in the Ocean, Journal of Geophysical Research: Oceans, 116, https://doi.org/10.1029/2011JC007342, 2011.

Zamanillo, M., Ortega-Retuerta, E., Nunes, S., Rodríguez-Ros, P., Dall'Osto, M., Estrada, M., Montserrat Sala, M., and Simó, R.: Main Drivers of Transparent Exopolymer Particle Distribution across the Surface Atlantic Ocean, Biogeosciences, 16, 733–749, https://doi.org/10.5194/bg-16-733-2019, 2019.

Zeppenfeld, S., van Pinxteren, M., Hartmann, M., Bracher, A., Stratmann, F., and Herrmann, H.: Glucose as a Potential Chemical Marker for Ice Nucleating Activity in Arctic Seawater and Melt Pond Samples, Environmental Science & Technology, 53, 8747–8756, https://doi.org/10.1021/acs.est.9b01469, 2019.